Rational design of amphiphilic BODIPY-based photosensitizers for multimodal imaging-guided phototherapy

Minling Jiang, Jinjin Zhang, Yaojun Li, Tingyu Shi, Tiantian Ma, Yiqi Sun, Huayu Qiu, Yang Li* and Shouchun Yin*

College of Material, Chemistry and Chemical Engineering, Hangzhou Normal University, Key Laboratory of Organosilicon Chemistry and Material Technology, Ministry of Education, Key Laboratory of Organosilicon Material Technology, Zhejiang Province, Hangzhou 310036, People's Republic of China

E-mail address: liyang@hznu.edu.cn, yinsc@hznu.edu.cn

Supporting Information

1. Materials and methods

All reagents were commercially available from Energy Chemical Company and used as supplied without further purification. The synthesis method of compound **1** can be referred to our previous work[S1]. Dulbecco's Modified Eagle Medium (DMEM) medium and Penicillin-Streptomycin were purchased from Gibco-BRL (Burlington, Canada). 3-(4,5-Dimethylthiazol-2-yl)-2,5-diphenyltetrazolium bromide (MTT), trypsine-EDTA, fetal bovine serum (FBS) and DAPI were purchased from Biomics Biotechnologies Co. Ltd. (Nantong, Jiangsu, China). The Reaction Oxygen Species Assay Kit and Calcein/PI Live/Dead Viability/Cytotoxicity Assay Kit were purchased from Beyotime Biotechnology (Shanghai, China).

^{1}H and ^{13}C nuclear magnetic resonance (NMR) spectra were collected on a Bruker Advance 500 MHz spectrometer with $CDCl_3$ as a deuterated solvent. Mass spectra were recorded on an Agilent Technologies 6530 Accurat-Mass Q-TOF LC/MS instrument. UV-vis absorption spectra were performed on Hitachi U-5300 absorption spectrophotometer. The fluorescent emission spectra were conducted on an Edinburgh FLS 980 fluorescence spectrophotometer. Dynamic light scattering (DLS) measurements were performed using a Nano ZS90 instrument equipped with a He-Ne laser (633 nm) and 90° collecting optics. Transmission electron microscopy (TEM) was performed on a Hitachi S-4800 and images were recorded on a Hitachi F-7700. Electron spin resonance (ESR) test was performed with JEOL JES-FA200. Optical Fiber Coupler laser (808 nm) was purchased from Ningbo Fingco Optoelectronic Co. Ltd. (Ningbo, China). Cellular fluorescence images were taken using a Nexcope NIB610-FL fluorescence microscope and a BIO-RAD Radiance 2100 confocal laser scanning microscope (CLSM). Flow cytometry data were obtained from CytoFLEX S. *In vivo* fluorescence images were performed with Monet IGS-1000.

2. Synthetic procedures and characterization data

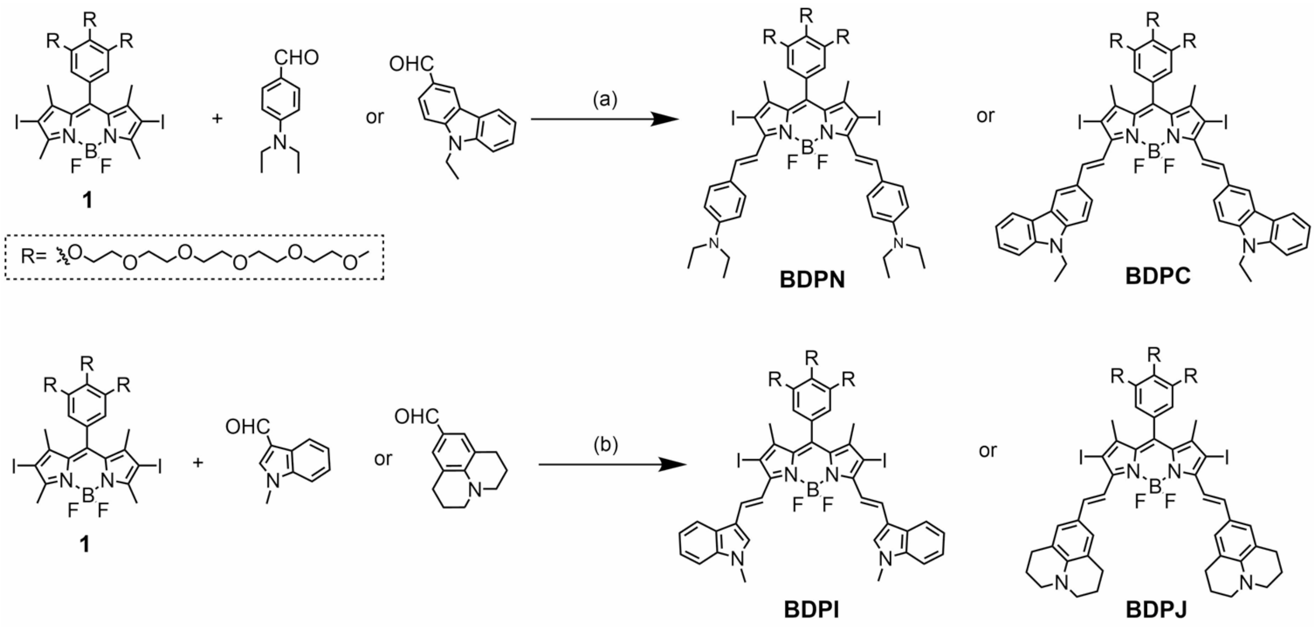

Scheme S1 The synthetic routes of compounds BDPN, BDPI, BDPC, BDPJ. Conditions: (a) piperidine, *p*-toluenesulfonic acid monohydrate, toluene, 120 °C, 12 h, 43% for BDPN, 13% for BDPC; (b) piperidine, acetic acid, toluene, 120 °C, 12~24 h, 29% for BDPC, 6% for BDPJ.

*2.1 Synthesis of compound **1***

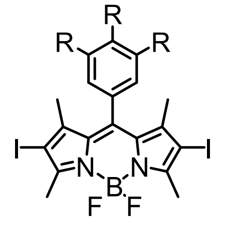

R= $O(CH_2CH_2O)_5CH_3$

Compound **1** was synthesized according to literature procedure[S1]. ^{1}H NMR (500 MHz, $CDCl_3$) δ (ppm): 6.50 (s, 2H), 4.25–4.20 (m, 2H), 4.13–4.08 (m, 4H), 3.85–3.80 (m, 6H), 3.72–3.58 (m, 42H), 3.54 (td, J = 6.5, 3.7 Hz, 6H), 3.37 (d, J = 5.5 Hz, 9H), 2.63 (s, 6H), 1.52 (s, 6H).

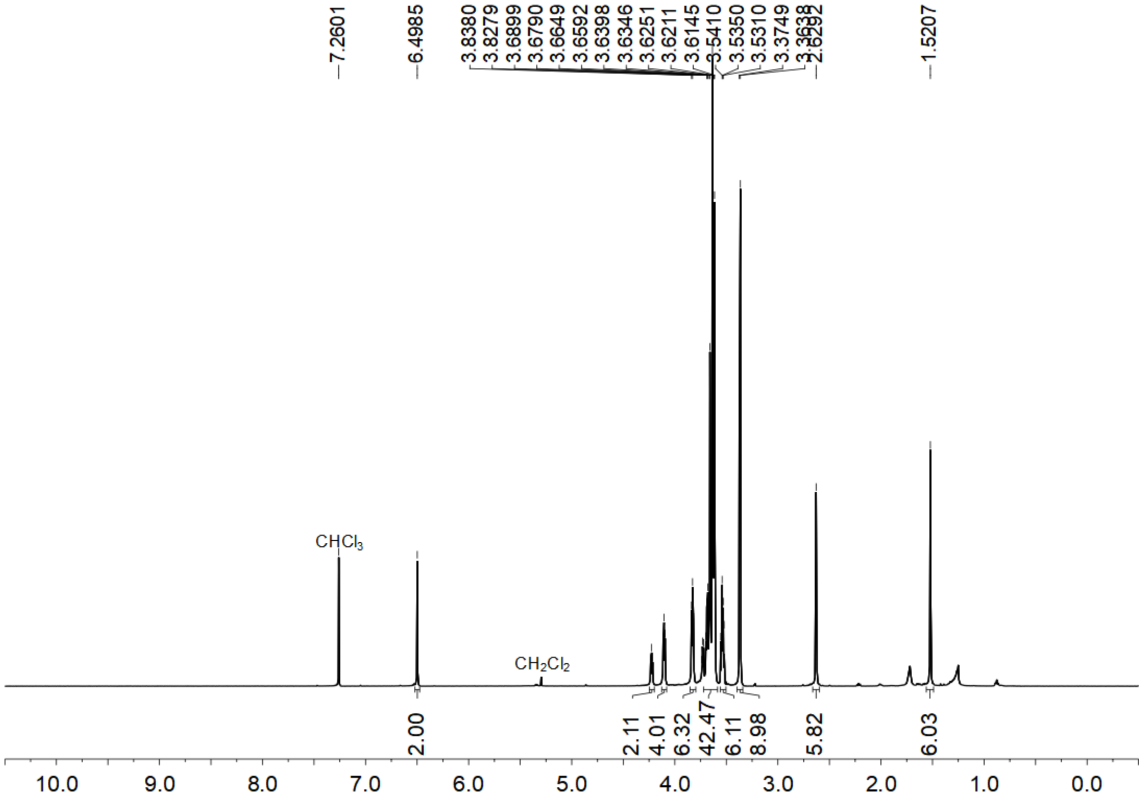

Fig. S1 ^{1}H NMR spectrum (500 MHz, $CDCl_3$, 298 K) of compound **1**.

2.2 Synthesis of compound BDPN

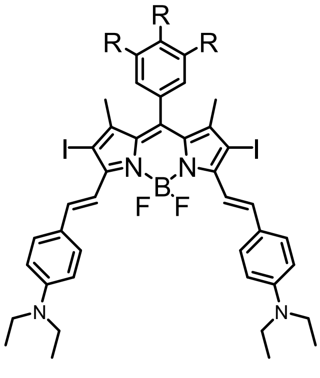

R= $O(CH_2CH_2O)_5CH_3$

N, *N*-Diethyl-4-aminobenzaldehyde (342 mg, 1.93 mmol) was added to a three-neck flask, compound **1** (640 mg, 0.48 mmol) was dissolved into 15 mL of dry toluene and added to the flask, followed by piperidine (520 µL, 5.68 mmol) and *p*-toluenesulfonic acid monohydrate (5.2 mg, 0.027 mmol). The mixed solution was heated to 120 ℃ under the protection of N_2, and the reaction progress was monitored by TLC. The mixture was cooled to room temperature, quenched with water and extracted with CH_2Cl_2. The crude product was purified by silica gel column chromatography (CH_2Cl_2/MeOH, 25:1, *v*/*v*) to obtain the final product of a black oily viscous substance (340 mg, 43%). ^{1}H NMR (500 MHz, $CDCl_3$) δ (ppm): 8.15 (d, J = 16.4 Hz, 2H), 7.52 (t, J = 7.8 Hz, 6H), 6.68 (d, J = 7.6 Hz, 4H), 6.54 (s, 2H), 4.27–4.22 (m, 2H), 4.15–4.11 (m, 4H), 3.86–3.82 (m, 6H), 3.73 (d, J = 4.5 Hz, 2H), 3.72–3.60 (m, 40H), 3.50 (m, 6H), 3.40 (q, J = 7.0 Hz, 8H), 3.36 (s, 3H), 3.34 (s, 6H), 1.55 (s, 6H), 1.19 (s, 12H). ^{13}C NMR (126 MHz, $CDCl_3$) δ (ppm): 153.7, 150.2, 148.6, 144.3, 139.6, 139.1, 132.6, 130.6, 129.6, 124.2, 113.7, 111.5, 108.3, 82.3, 72.7, 71.8, 71.8, 70.8, 70.5, 69.7, 69.1, 58.9, 58.9, 44.5, 17.3, 12.6. ^{19}F NMR (471 MHz, $CDCl_3$) δ (ppm): −139.23

(dd, J = 66.8, 31.8 Hz, BF$_2$). ESI-HRMS [M + Na]$^+$: calcd. For [C$_{74}$H$_{109}$BF$_2$I$_2$N$_4$O$_{18}$Na]$^+$ 1667.5792, found 1667.5868.

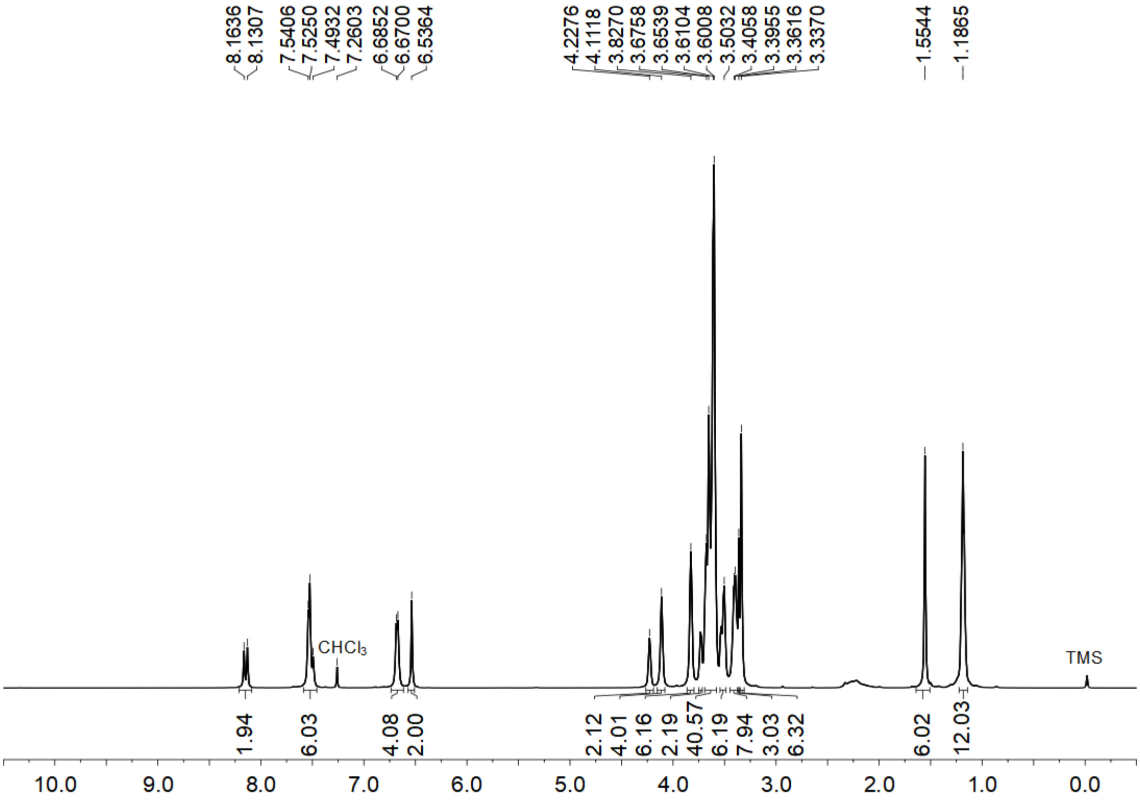

Fig. S2. ^{1}H NMR spectrum (500 MHz, CDCl$_3$, 298 K) of compound BDPN.

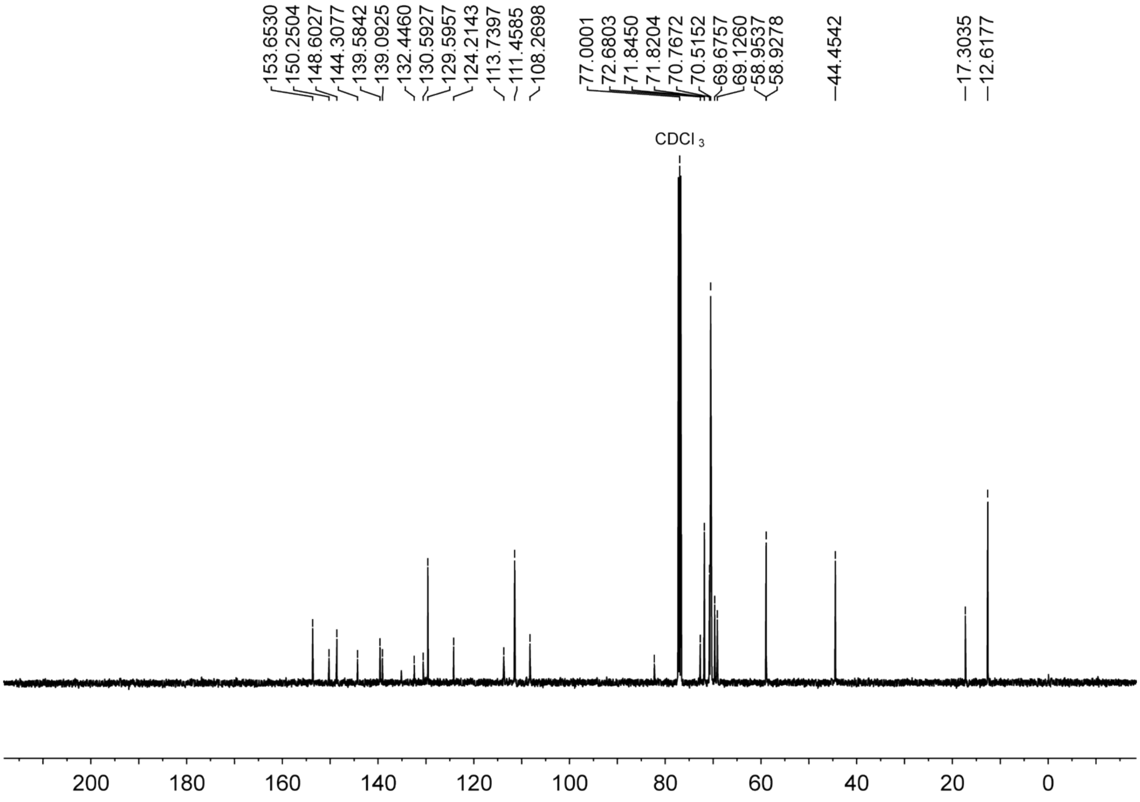

Fig. S3 ^{13}C NMR spectrum (126 MHz, CDCl$_3$, 298 K) of compound BDPN.

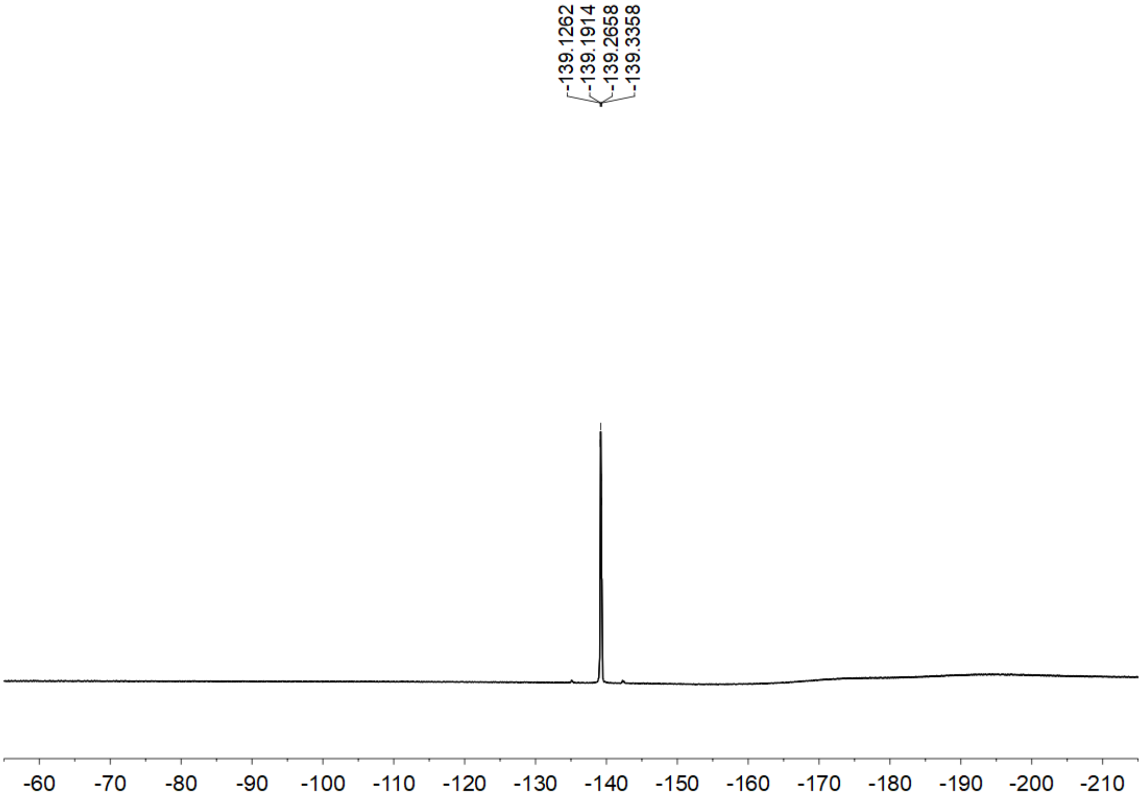

Fig. S4 ^{19}F NMR spectrum (471 MHz, $CDCl_3$, 298 K) of compound BDPN.

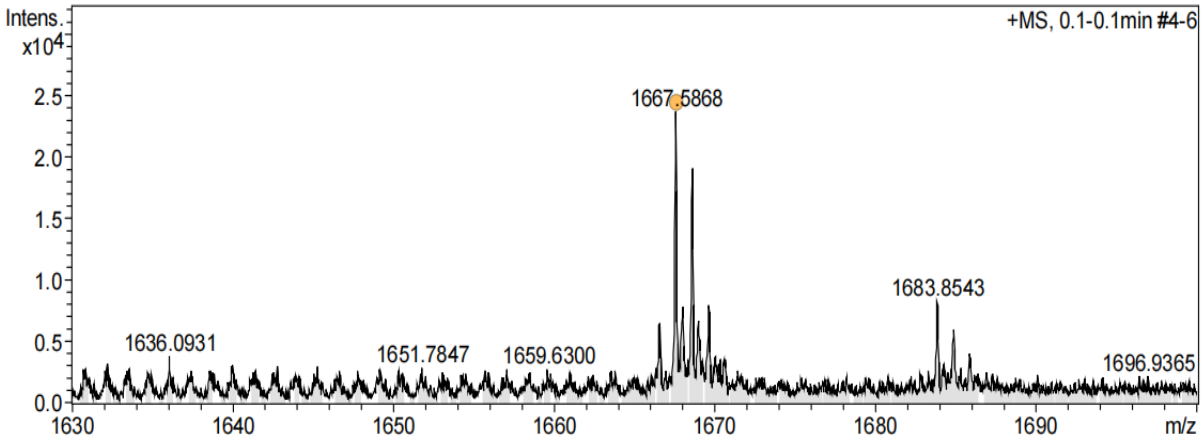

Fig. S5 ESI-HRMS spectrum of compound BDPN.

2.3 Synthesis of compound BDPI

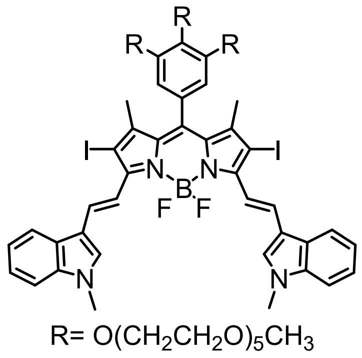

1-Methylindole-3-carboxaldehyde (48 mg, 0.3 mmol) was added to a three-neck flask, compound **1** (100 mg, 0.075 mmol) was dissolved into 15 mL of dry toluene and added to the flask, followed by piperidine (84 μL, 0.92 mmol) and acetic acid (84 μL, 1.47 mmol). The mixed solution was heated to 120 °C under the protection of N_2, and the reaction progress was monitored by TLC. The mixture was cooled to room temperature, quenched with water and extracted with CH_2Cl_2. The crude product was purified by silica gel column chromatography (CH_2Cl_2/MeOH, 20:1, *v*/*v*) to obtain the final product of a black oily viscous substance (16 mg, 13%). ^{1}H NMR (500 MHz, $CDCl_3$) δ (ppm): 8.50 (d, J = 16.6 Hz, 2H), 8.18 (d, J = 7.9 Hz, 2H), 7.80 (d, J = 16.6 Hz, 2H), 7.46 (s, 2H), 7.33 (ddd, J = 10.6, 8.8, 4.4 Hz, 4H), 7.28–7.24 (m, 2H), 6.59 (s, 2H), 4.27–4.23 (m, 2H), 4.16–4.12 (m, 4H), 3.85 (dd, J = 6.7, 2.7 Hz, 6H), 3.83 (s, 6H), 3.73–3.59 (m, 42H), 3.56 (dd, J = 5.7, 3.7 Hz, 2H), 3.54–3.49 (m, 4H), 3.38 (s, 3H), 3.35 (s, 6H), 1.60 (s, 6H). ^{13}C NMR (126 MHz, $CDCl_3$) δ (ppm): 153.7, 150.4, 144.3, 139.1, 138.1, 135.1, 132.6, 132.5, 131.7, 130.6, 126.2, 122.7, 121.3, 120.9, 114.9, 114.8, 109.7, 108.3, 82.2, 72.7, 71.9, 71.8, 70.8, 70.6, 70.5, 70.5, 70.5, 70.5, 70.4, 70.4, 69.7, 69.2, 59.0, 58.9, 33.1, 29.6, 17.3. ^{19}F NMR (471 MHz, $CDCl_3$) δ (ppm): −139.59 (dd, J = 67.9, 32.6 Hz, BF_2). ESI-HRMS $[M + Na]^+$: calcd. for $[C_{72}H_{97}[11B]F_2I_2N_4O_{18}Na]^+$ 1631.4841, found 1631.4827.

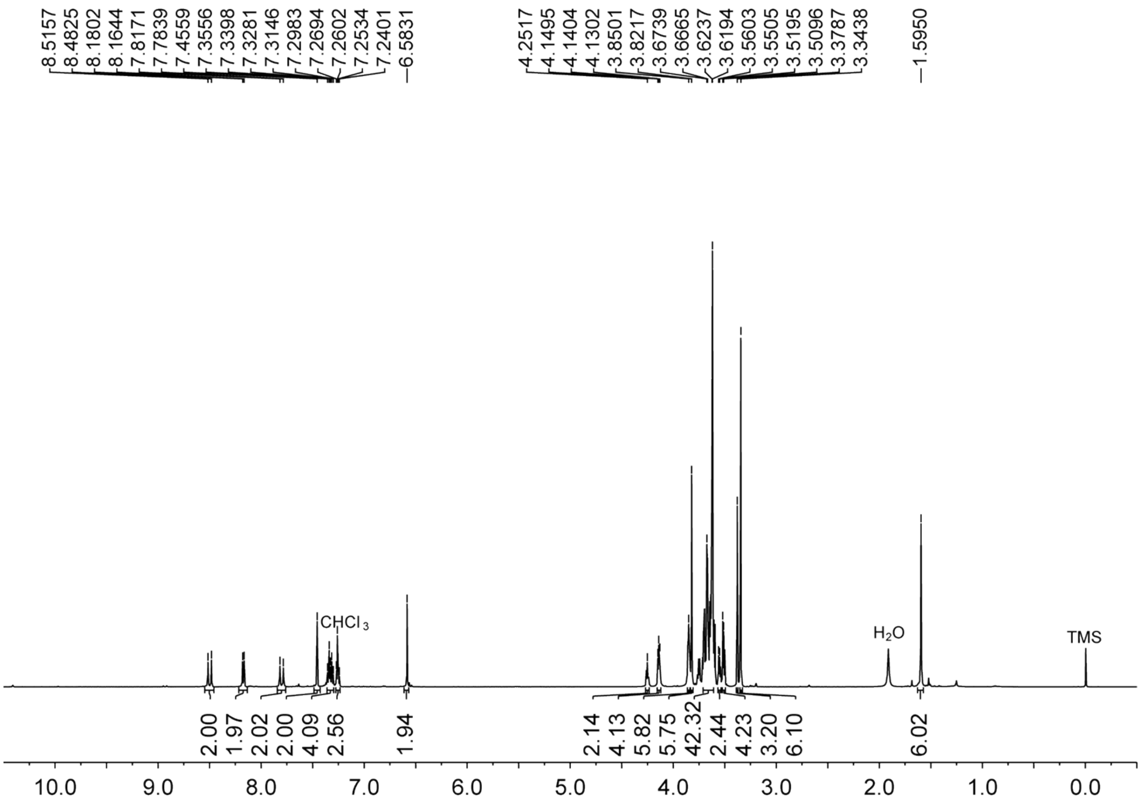

Fig. S6 ^{1}H NMR spectrum (500 MHz, $CDCl_3$, 298 K) of compound BDPI.

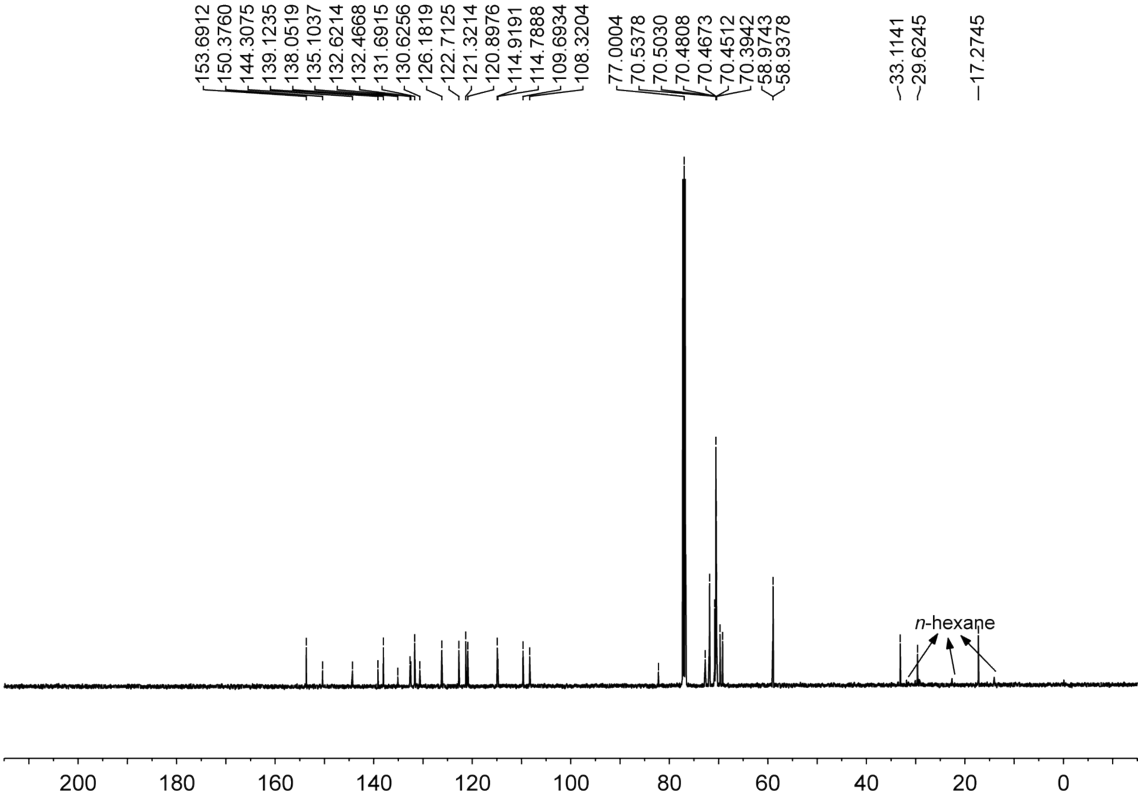

Fig. S7 ^{13}C NMR spectrum (126 MHz, $CDCl_3$, 298 K) of compound BDPI.

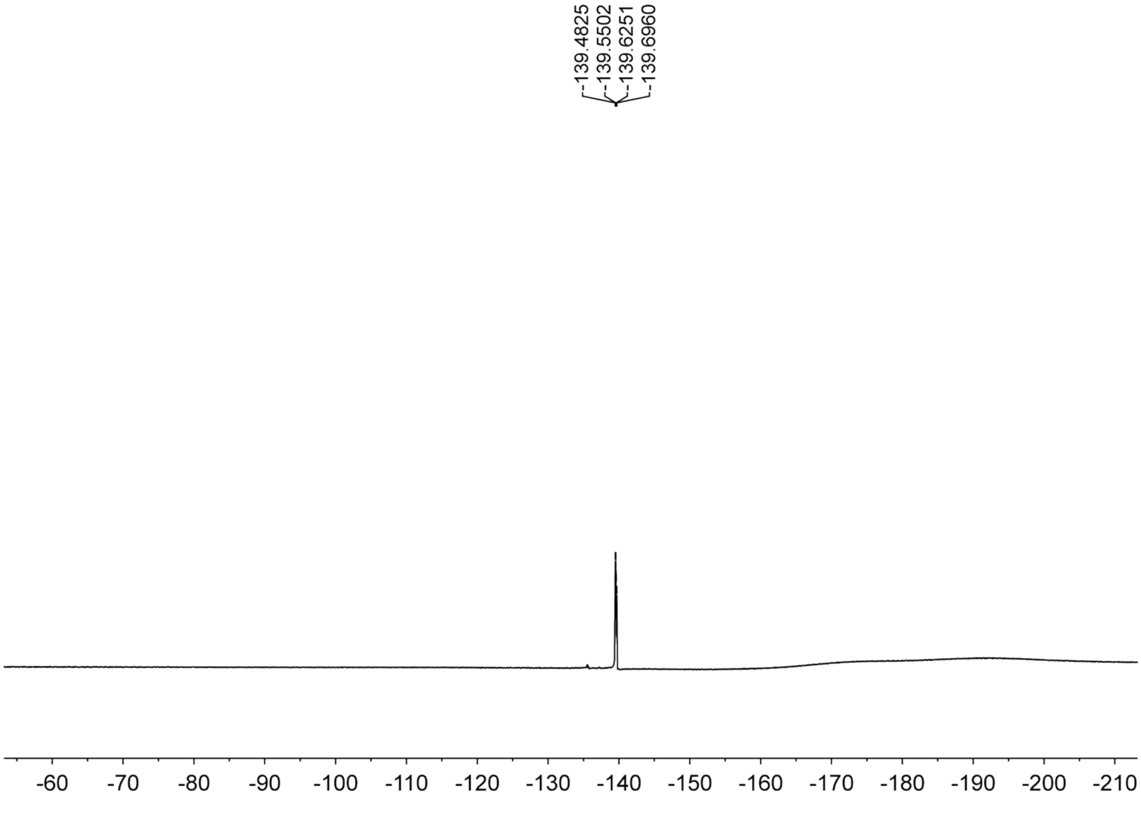

Fig. S8 ^{19}F NMR spectrum (471 MHz, $CDCl_3$, 298 K) of compound BDPI.

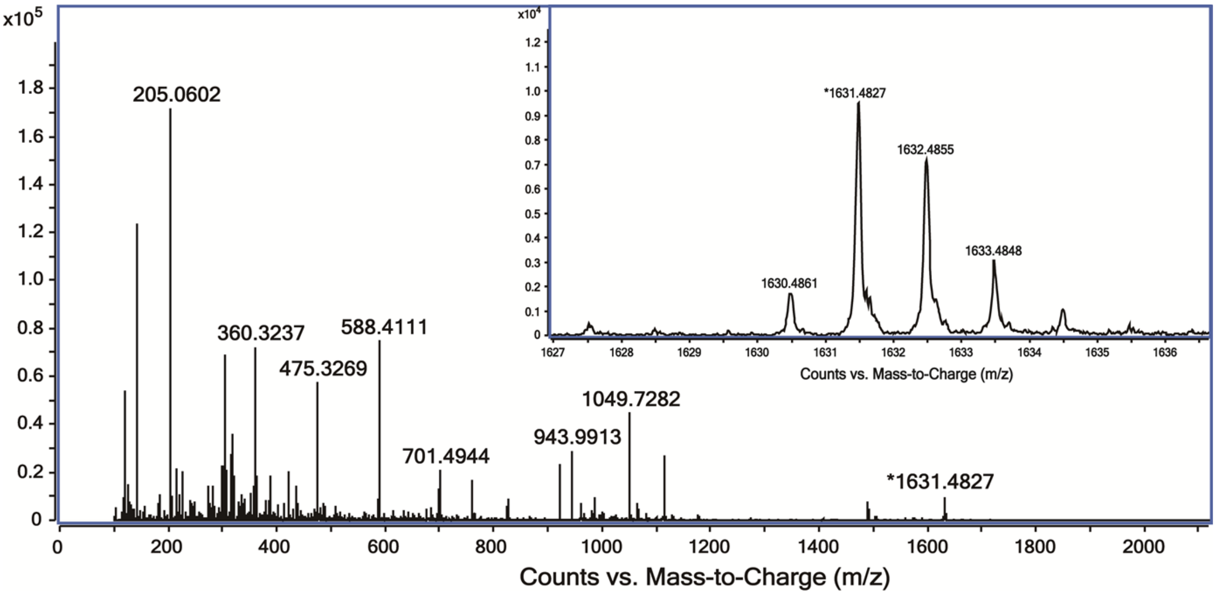

Fig. S9 ESI-HRMS spectrum of compound BDPI.

2.4 Synthesis of BDPC

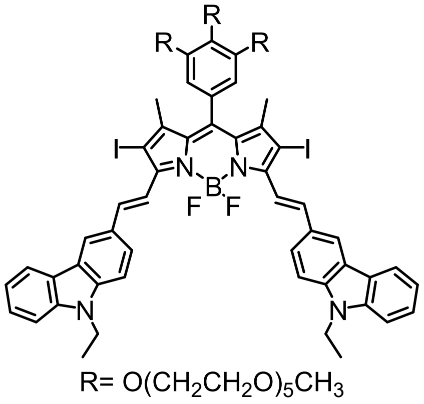

N-Ethyl-3-carbazolecarboxaldehyde (100 mg, 0.45 mmol) was added to a three-neck flask, compound **1** (150 mg, 0.11 mmol) was dissolved into 15 mL of dry toluene and added to the flask, followed by piperidine (122 μL, 1.33 mmol) and *p*-toluenesulfonic acid monohydrate (1.2 mg, 0.0064 mmol). The mixed solution was heated to 120 °C under the protection of N_2, and the reaction progress was monitored by TLC. The mixture was cooled to room temperature, quenched with water and extracted with CH_2Cl_2. The crude product was purified by silica gel column chromatography (CH_2Cl_2/MeOH, 20:1, *v*/*v*) to obtain the final product of a black oily viscous substance (57 mg, 29%). ^{1}H NMR (500 MHz, $CDCl_3$) δ (ppm): 8.44 (d, J = 16.5 Hz, 2H), 8.36 (s, 2H), 8.18 (d, *J* = 7.7 Hz, 2H), 7.89 (d, *J* = 8.5 Hz, 2H), 7.80 (d, *J* = 16.6 Hz, 2H), 7.47 (dt, *J* = 16.8, 8.0 Hz, 6H), 7.24 (t, *J* = 7.4 Hz, 2H), 6.60 (s, 2H), 4.40 (dd, *J* = 14.3, 7.1 Hz, 4H), 4.30–4.24 (m, 2H), 4.22–4.11 (m, 4H), 3.92–3.84 (m, 6H), 3.80–3.59 (m, 42H), 3.54 (ddd, *J* = 18.2, 5.6, 3.7 Hz, 6H), 3.39 (s, 4H), 3.35 (s, 4H), 1.63 (s, 6H), 1.47 (t, *J* = 7.2 Hz, 6H). ^{13}C NMR (126 MHz, $CDCl_3$) δ (ppm): 153.8, 150.5, 145.1, 140.7, 140.3, 139.2, 136.9, 132.7, 130.3, 127.9, 125.9, 125.4, 123.4, 123.0, 120.8, 120.7, 119.4, 116.0, 108.8, 108.7, 108.0, 82.7, 72.7, 71.8, 71.8, 70.8, 70.6, 70.5, 70.5, 70.4, 70.4, 69.7, 69.2, 58.9, 58.9, 37.6, 17.4, 13.8. ^{19}F NMR (471 MHz, $CDCl_3$, 298 K) δ (ppm): −138.81 (dd, *J* = 66.6, 31.9 Hz, BF_2). ESI-HRMS $[M + Na]^+$: calcd. for $[C_{82}H_{105}BF_2I_2N_4O_{18}Na]^+$ 1759.5480, found 1759.5578.

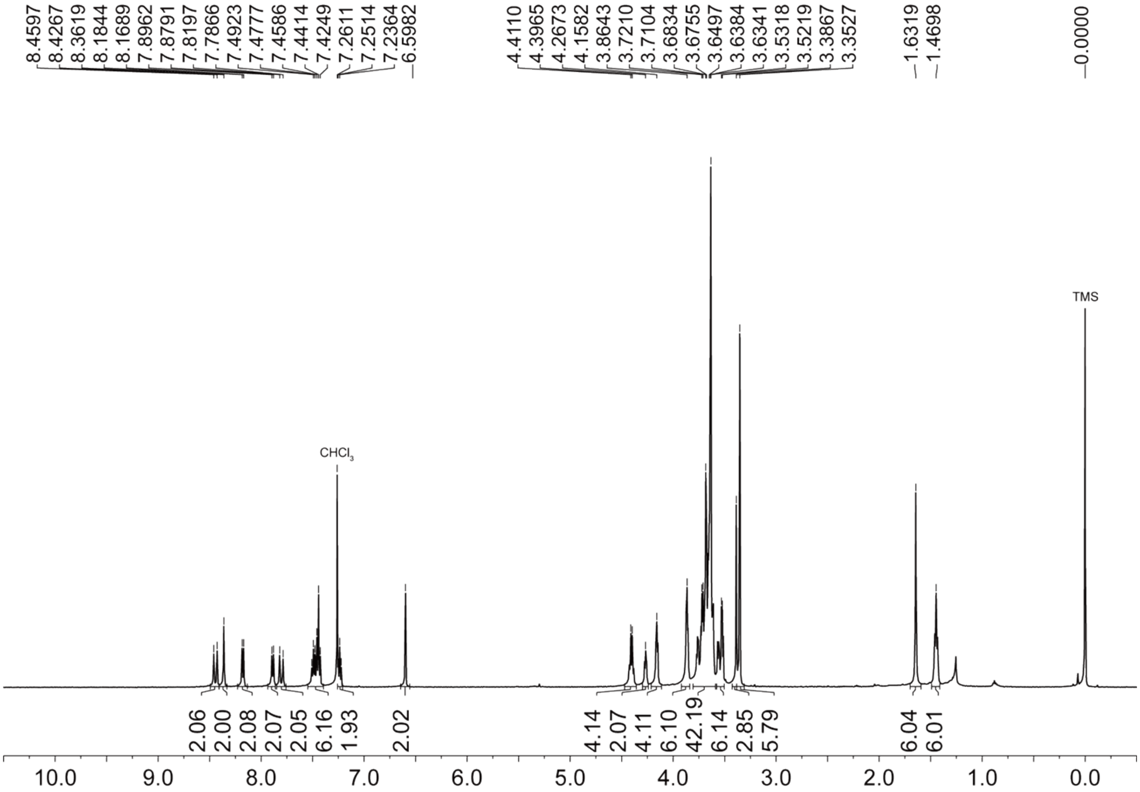

Fig. S10 ^{1}H NMR spectrum (500 MHz, CDCl$_3$, 298 K) of compound BDPC.

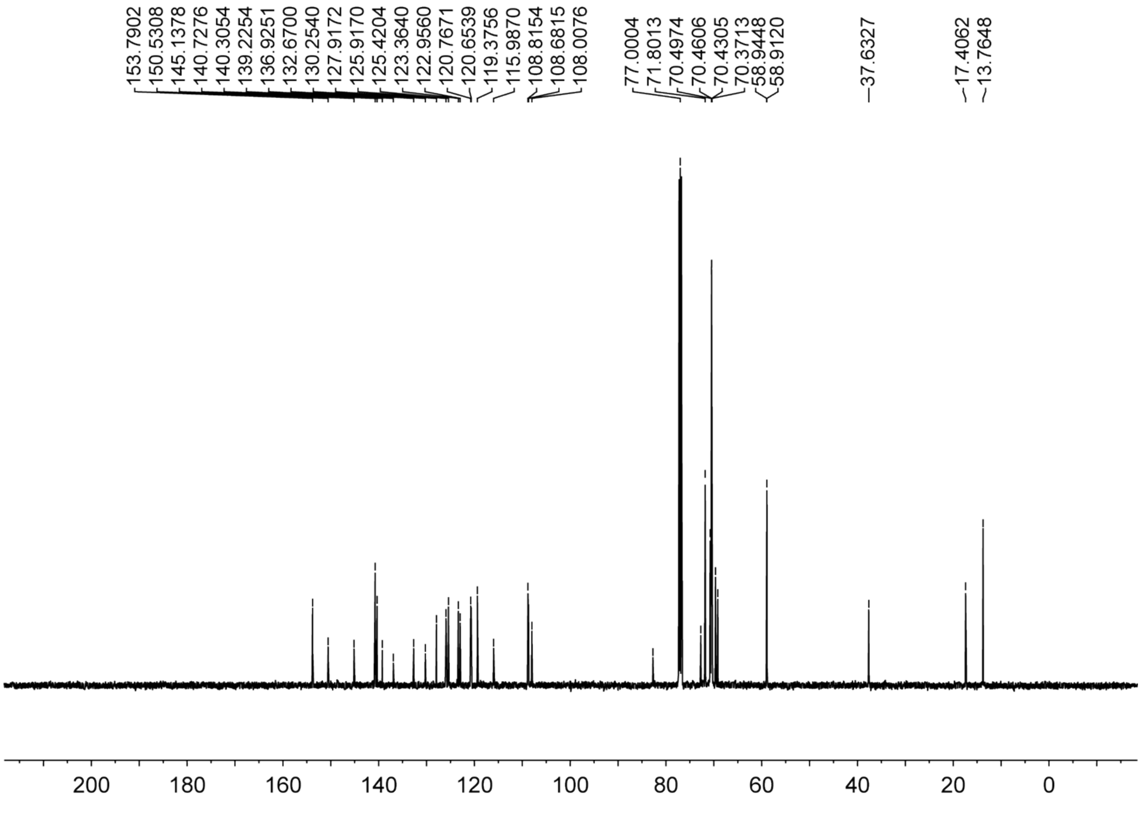

Fig. S11 ^{13}C NMR spectrum (126 MHz, CDCl$_3$, 298 K) of compound BDPC.

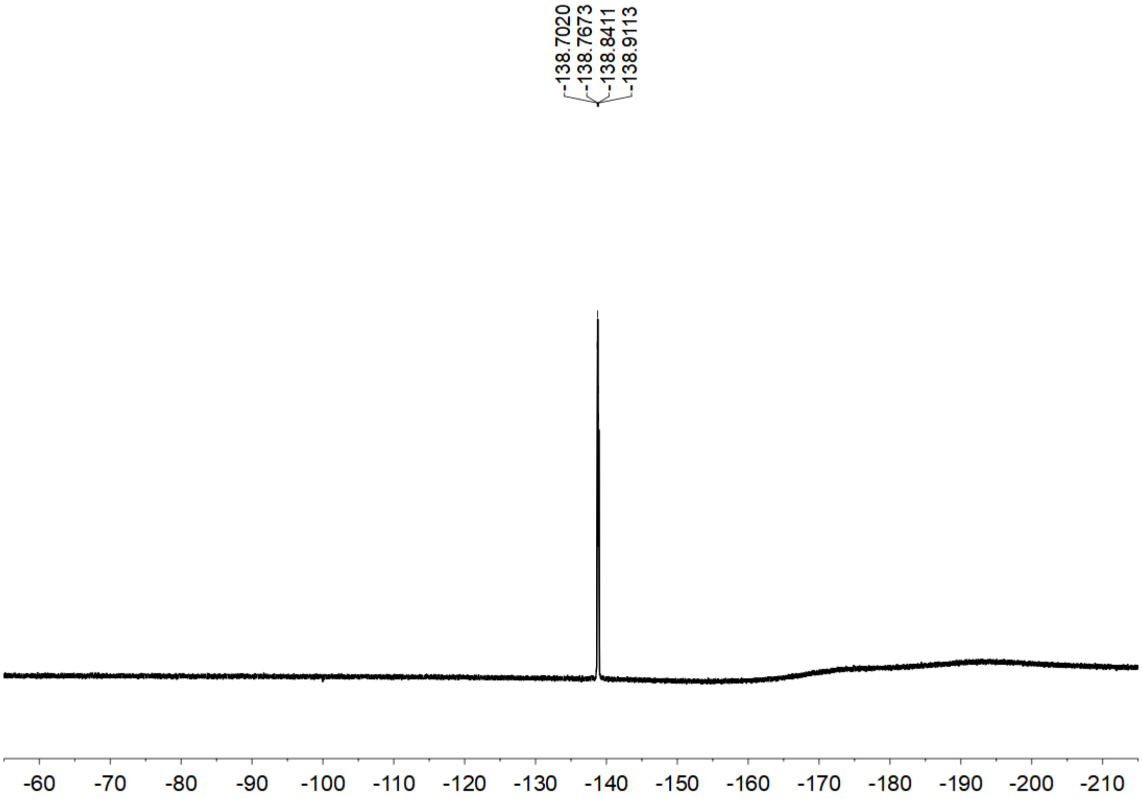

Fig. S12 ^{19}F NMR spectrum (471 MHz, $CDCl_3$, 298 K) of compound BDPC.

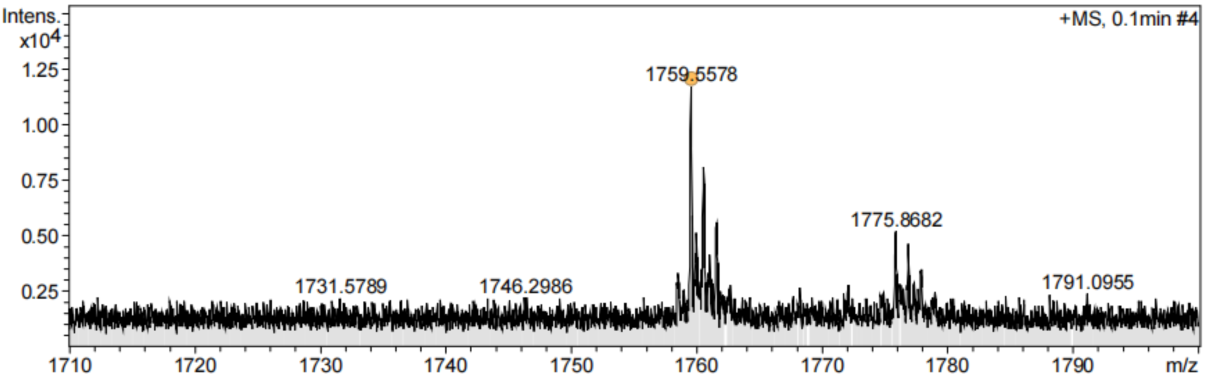

Fig. S13 ESI-HRMS spectrum of compound BDPC.

2.5 Synthesis of compound BDPJ

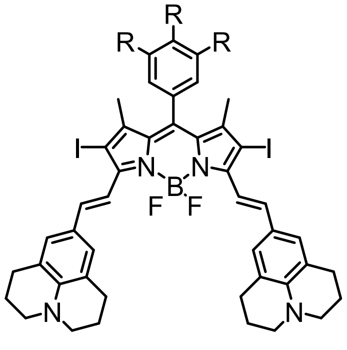

R= $O(CH_2CH_2O)_5CH_3$

9-Julolidinecarboxaldehyde (60 mg, 0.3 mmol) was added to a three-neck flask, compound **1** (100 mg, 0.075 mmol) was dissolved into 15 mL of dry toluene and added to the flask, followed by piperidine (84 μL, 0.92 mmol) and acetic acid (84 μL, 1.47 mmol). The mixed solution was heated to 120 °C under the protection of N_2, and the reaction progress was monitored by TLC. The mixture was cooled to room temperature, quenched with water and extracted with CH_2Cl_2. The crude product was purified by silica gel column chromatography (CH_2Cl_2/MeOH, 20:1, *v*/*v*) to obtain the final product of a black oily viscous substance (8 mg, 6%). ^{1}H NMR (500 MHz, $CDCl_3$) δ (ppm):

8.06 (d, J = 16.5 Hz, 2H), 7.45 (d, J = 16.5 Hz, 2H), 7.11 (s, 4H), 6.54 (s, 2H), 4.27–4.20 (m, 2H), 4.16–4.09 (m, 4H), 3.85–3.80 (m, 6H), 3.75–3.60 (m, 42H), 3.56–3.51 (m, 6H), 3.37 (d, J = 11.1 Hz, 9H), 3.31–3.14 (m, 8H), 2.79 (t, J = 6.1 Hz, 8H), 1.98 (dd, J = 11.2, 5.6 Hz, 8H), 1.55 (s, 6H). ^{13}C NMR (126 MHz, CDCl$_3$) δ (ppm): 153.6, 150.2, 144.1, 144.0, 140.0, 139.0, 134.5, 132.4, 130.7, 130.7, 127.1, 124.1, 121.1, 113.3, 108.3, 108.3, 82.4, 72.7, 71.9, 71.8, 70.8, 70.6, 70.5, 70.5, 70.5, 70.4, 69.7, 69.1, 59.0, 50.0, 29.6, 27.7, 21.7, 17.3. ^{19}F NMR (471 MHz, CDCl$_3$) δ (ppm): −139.42 (dd, J = 67.2, 32.2 Hz, BF$_2$). ESI-HRMS $[M + Na]^+$: calcd. for $[C_{78}H_{109}[11B]F_2I_2N_4O_{18}Na]^+$ 1715.578, found 1715.5779.

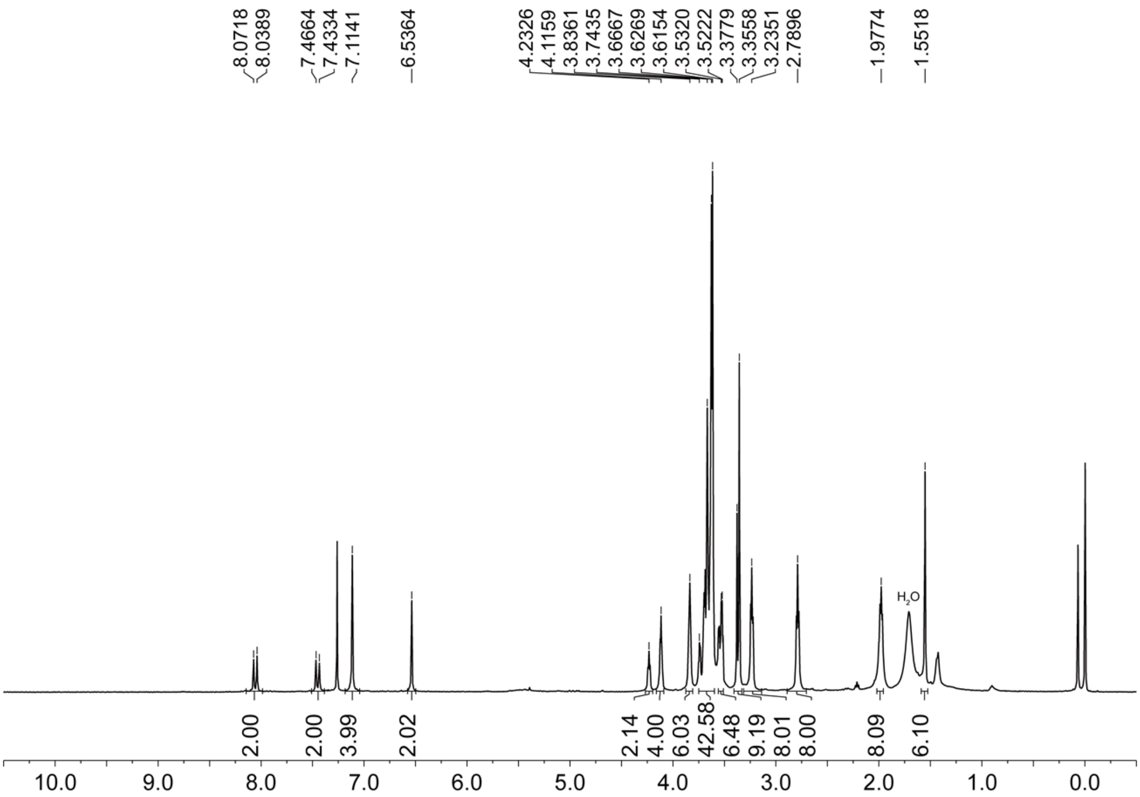

Fig. S14 ^{1}H NMR spectrum (500 MHz, CDCl$_3$, 298 K) of compound BDPJ.

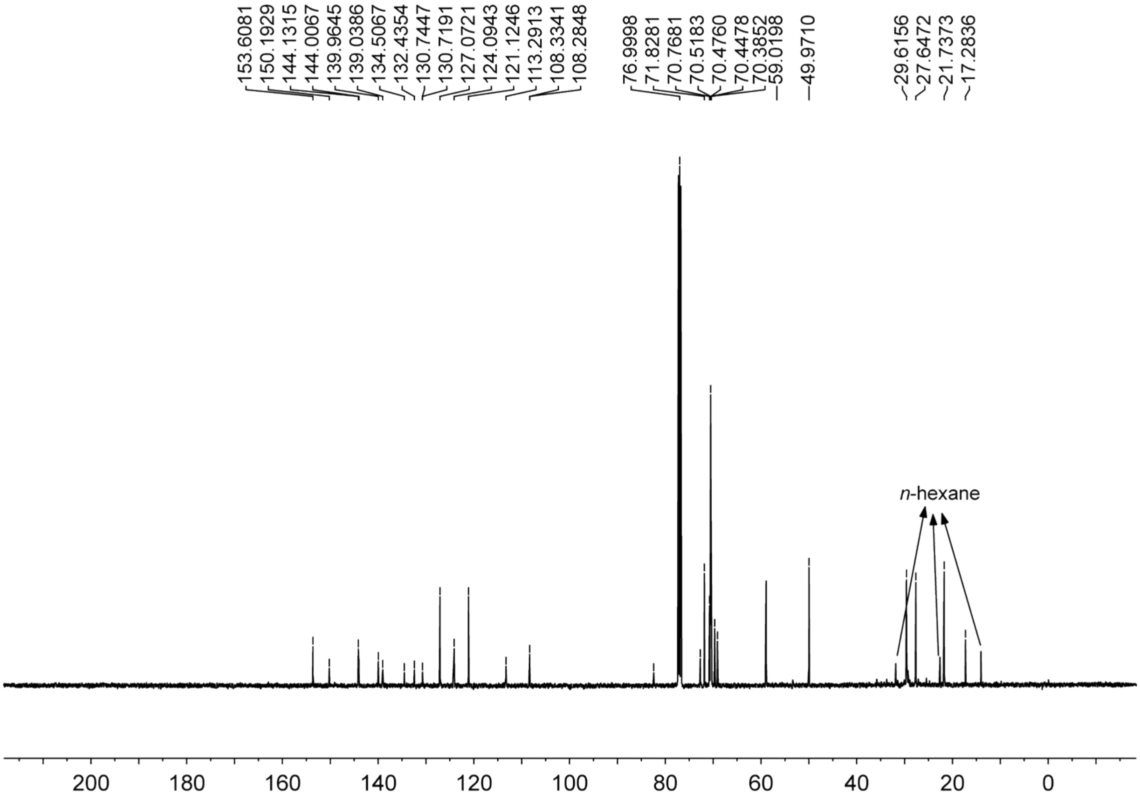

Fig. S15 ^{13}C NMR spectrum (126 MHz, CDCl$_3$, 298 K) of compound BDPJ.

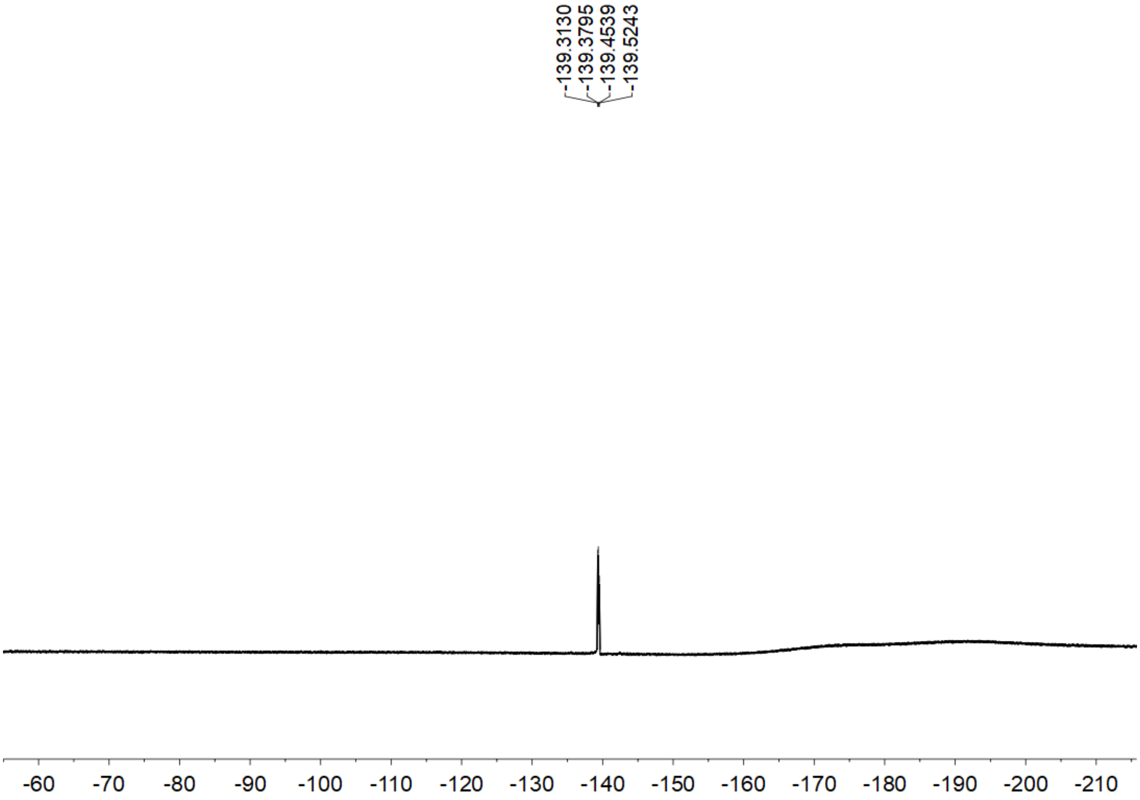

Fig. S16 ^{19}F NMR spectrum (471 MHz, CDCl$_3$, 298 K) of compound BDPJ.

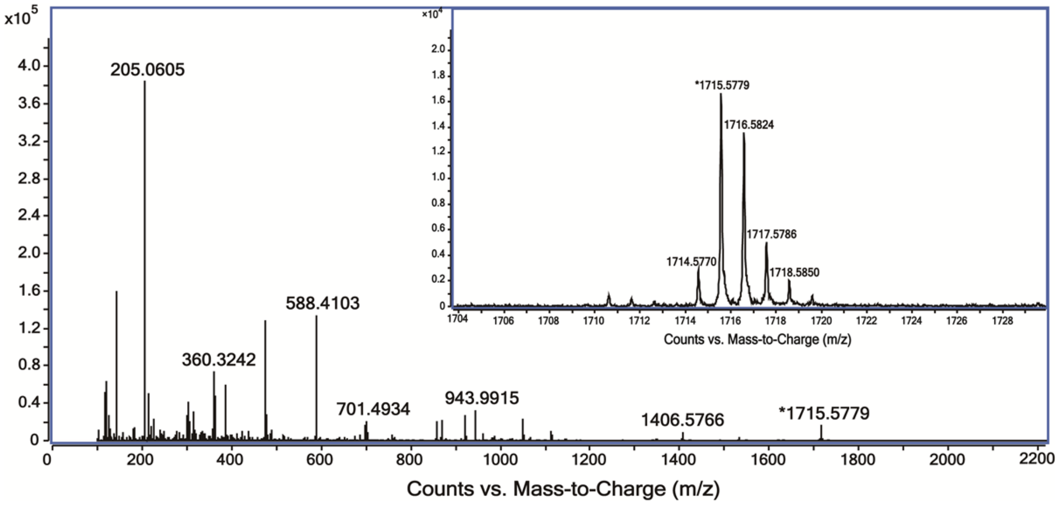

Fig. S17 ESI-HRMS spectrum of compound BDPJ.

3. Determination of CAC values of BDPN, BDPI, BDPC, BDPJ

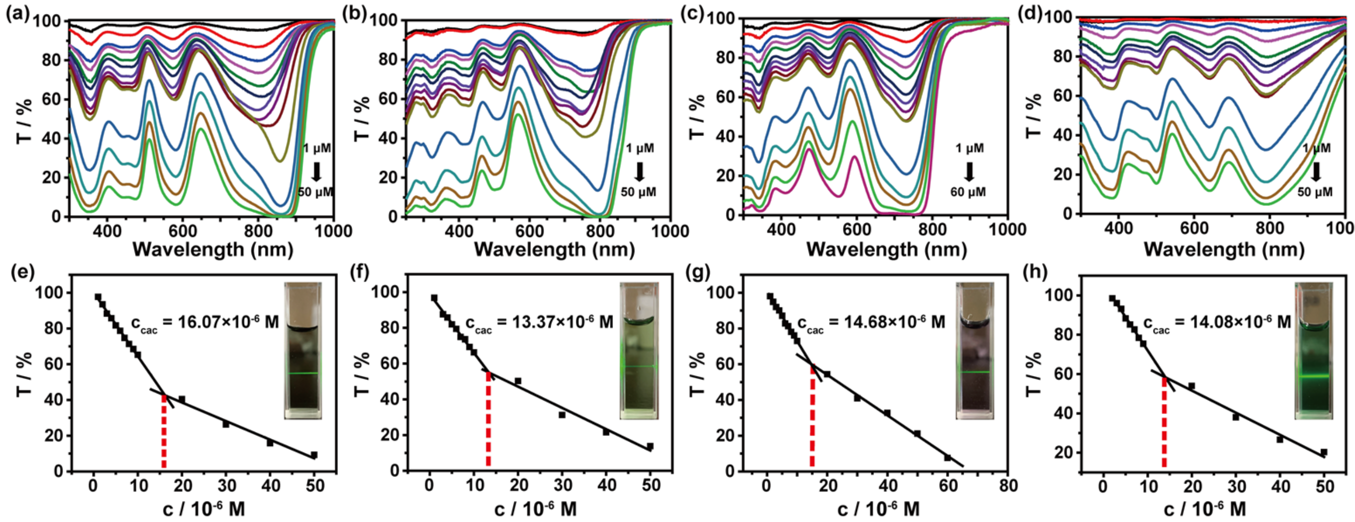

Fig. S18 Optical transmittance of aqueous solution of (a) BDPN, (b) BDPI, (c) BDPC and (d) BDPJ with different concentrations. CAC of (e) BDPN, (f) BDPI, (g) BDPC and (h) BDPJ aqueous solutions. Inset: images for the Tyndall effect.

4. Absorption changes of BDPI, BDPC, BDPJ

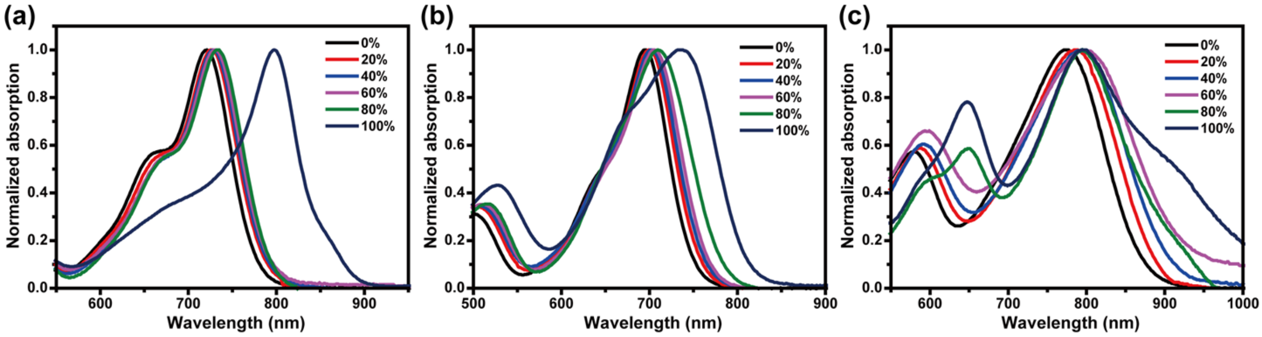

Fig. S19 UV-vis spectra of (a) BDPI, (b) BDPC and (c) BDPJ (10 μM) in THF/water mixtures (Labeled as water content).

5. Density functional theory (DFT) calculations of BDPN, BDPI, BDPC, BDPJ

All-electron DFT calculations have been carried out by the latest version of ORCA quantum chemistry softwarei (Version 5.0.3). For geometry optimization calculations, BLYP general functions and def2-SVP basis sets were used and the optimal geometry for each compound was determined.The DFT-D3 dispersion correction with BJ-damping was applied to correct the weak interaction to improve the calculation accuracy. The excited states and Spin-Orbit Coupling (SOC) calculations were performed with B3LYP functional and the mixed basis set (SARC-DKH-TZVP basis setii for I atom and DKH-def2-SVP basis set for other atoms). Orbital energy level analysis was performed by multiwfn software. SOC calculation was performed by spin-orbit mean-field (SOMF) method. Orbital energy level analysis was performed by Multiwfn software.

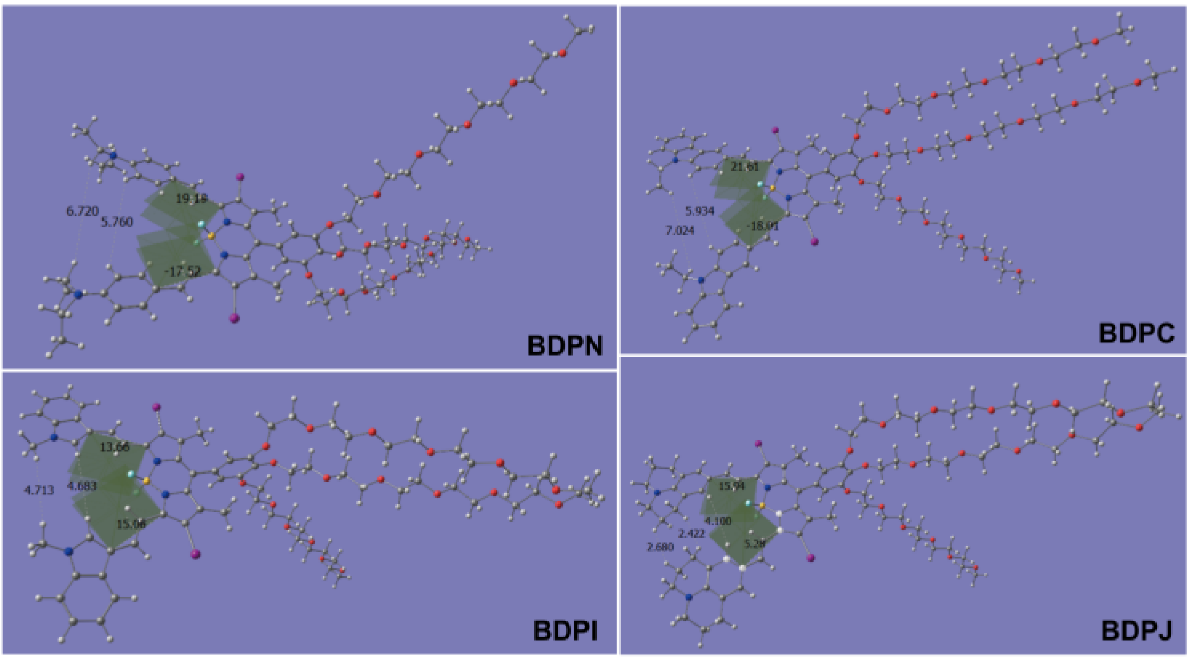

Fig. S20 The optimized geometry and dihedral angle between the group and the BODIPY nucleus from DFT calculations of *BDPN, BDPI, BDPC, BDPJ*.

Table S1 Photophysical and photosensitizing properties of BDP dyes.

Compounds	S_1 / eV	T_1 / eV	ΔE_{ST} / eV
BDPN	1.827	0.931	0.896
BDPI	1.880	0.888	0.992
BDPC	1.870	0.972	0.898
BDPJ	1.688	0.858	0.830

6. Preparation of nanoparticles

BDPN/BDPI/BDPC/BDPJ nanoparticles (NPs) were prepared by nanoprecipitation. Initially, BDPN/BDPI/BDPC/BDPJ (1 mg) was dissolved in 0.8 mL of THF. Subsequently, the solution was slowly dropped into deionized water (30 mL), and the mixture was vigorously stirred at room temperature for overnight. The formed NPs solution was concentrated under low temperature and pressure for further applications.

7. DLS and TEM Analysis of BDPN/BDPI/BDPC/BDPJ NPs

BDPN/BDPI/BDPC/BDPJ NPs (20 μM) were measured in a quartz cuvette after equilibrating for 15 min at 25 ℃. In addition, 10 μL of BDPN/BDPI/BDPC/BDPJ NPs (20 μM) was deposited on the ultra-thin carbon film and left to dry overnight and dried at 50℃ for half an hour before TEM analysis.

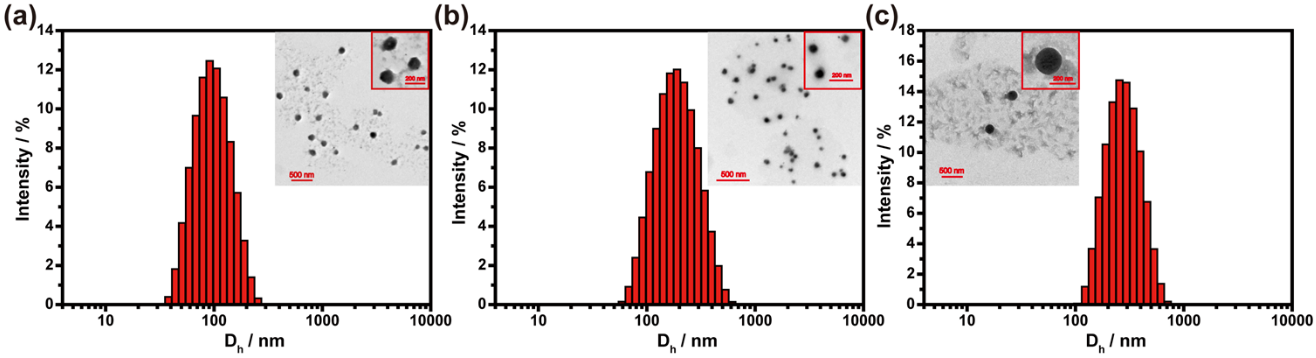

Fig. S21 Size distribution of (a) BDPI NPs, (b) BDPC NPs, (c) BDPJ NPs using DLS (Inset: TEM image of NPs).

8. Fluorescence quantum yield measurement

The fluorescence quantum yields of BDPN, BDPI, BDPC, BDPJ (in CH_2Cl_2) and BDPN NPs, BDPI NPs, BDPC NPs, BDPJ NPs (in water) were measured by the integrating sphere method. The maximum absorbance of the solution should be controlled below 0.1. The data could be obtained from Edinburgh FLS 980 fluorescence spectrophotometer.

9. Electron Spin Resonance (ESR) Spectra of four NPs in solution

The species of reactive oxygen species was determined by ESR spectrometer. The production of the singlet oxygen ($^1O_2$), ·OH radical and $O_2^{-\cdot}$ radical was determined using 2,2,6,6-tetramethylpiperidine (TEMP) and 5,5-dimethyl-1-pyrrolin-1-oxide (DMPO) as spin trapping agents, respectively. ESR spectrometer was used to track the changes of the mixtures of four NPs and TEMP/DMPO before and after 10 min of 808 nm laser irradiation.

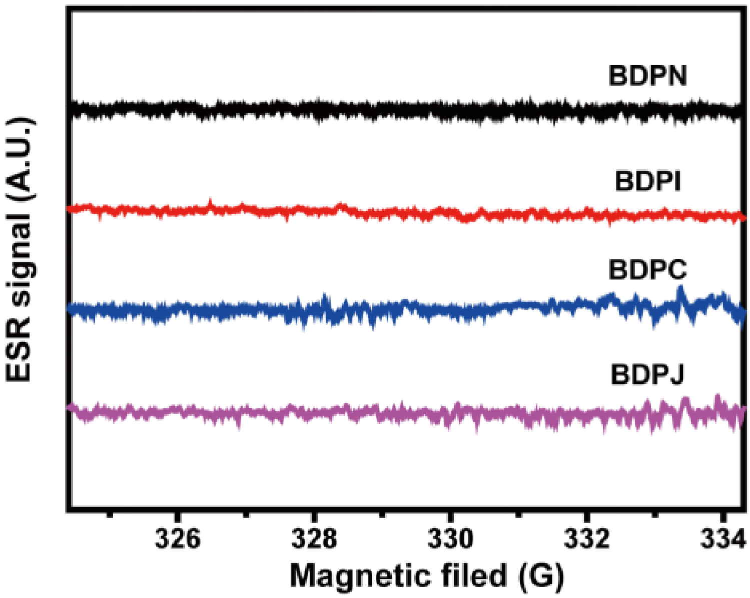

Fig. S22 ESR spectra of BDPN NPs BDPI NPs BDPC NPs or BDPJ NPs in the presence of DMPO under 808 nm irradiation.

10. Singlet Oxygen Production

As a singlet oxygen trapping agent, DPBF can be used to compare the ability of four nanoparticles to generate $^1O_2$ in aqueous solution. In simple terms, 100 µL of DPBF (1.0 mM in THF) and 500 µL of BDPN/BDPI/BDPC/BDPJ NPs (20 µM in aqueous solution) were added to 1.4 mL of water and stirred well. After 808 nm irradiation at 0.1 W cm^{-2}, the absorbances of DPBF at 415 nm were recorded by UV-vis spectrophotometer at an interval of 10 s. Subsequently, 100 µL of DPBF (1.0 mM in THF) and 100, 200, 300, 400, 500 µL of BDPN NPs (20 µM in aqueous solution) were added to 1.8, 1.7, 1.6, 1.5, 1.4 mL of water and stirred well. Upon 808 nm irradiation at 0.1 W cm^{-2}, the absorbances of DPBF at 415 nm were recorded by UV-vis spectrophotometer at an interval of 10 s. Then, 100 µL of DPBF (1.0 mM in THF) and 100 µL of BDPN NPs (20 µM in aqueous solution) were added to 1.8 mL of water and stirred well. Upon 808 nm irradiation with different powers (0.1, 0.2, 0.3, 0.4, 0.5 W cm^{-2}), the absorbance of DPBF at 415 nm was recorded by UV-vis spectrophotometer at an interval of 10 s. Finally, photostability of the four NPs was explored through UV-vis spectrophotometer upon 808 nm laser irradiation (0.5 W cm^{-2}) in an interval of 1 min.

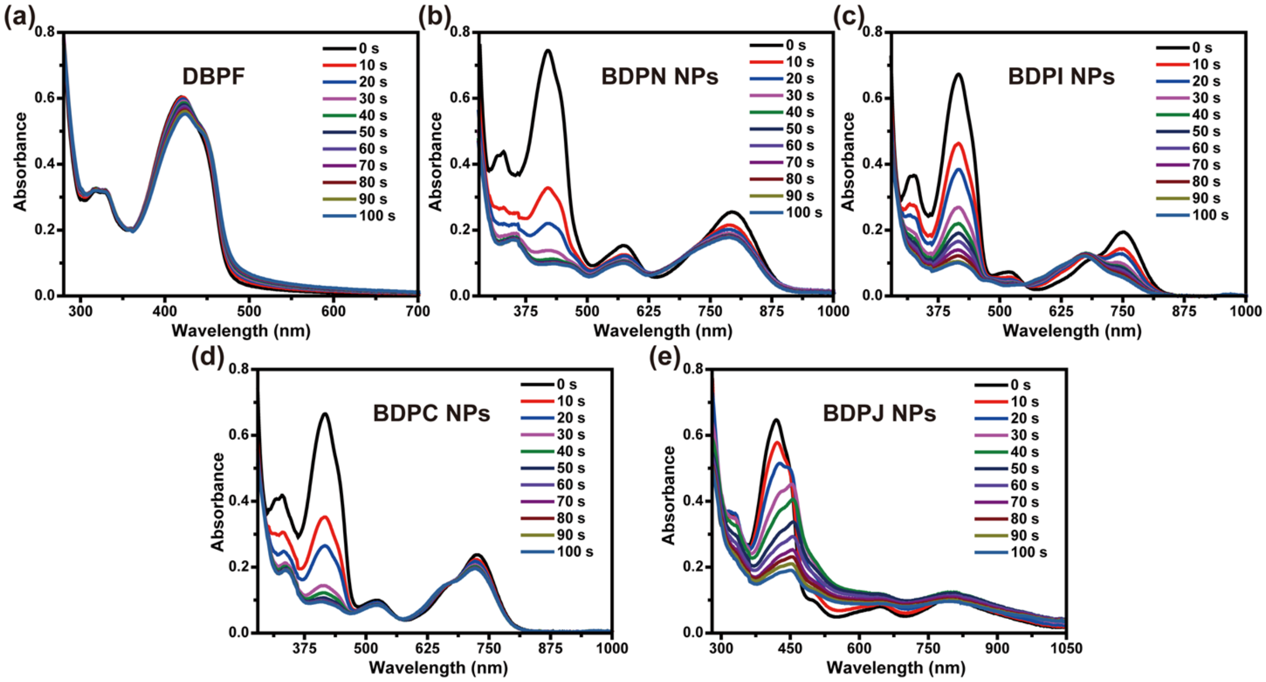

Fig. S23 UV-vis spectra of (a) DPBF alone, or the same concentration of (b) BDPN NPs, (c) BDPI NPs, (d) BDPC NPs, (e) BDPJ NPs and DPBF in the presence of 808 nm laser irradiation (0.1 W cm^{-2}) at different times.

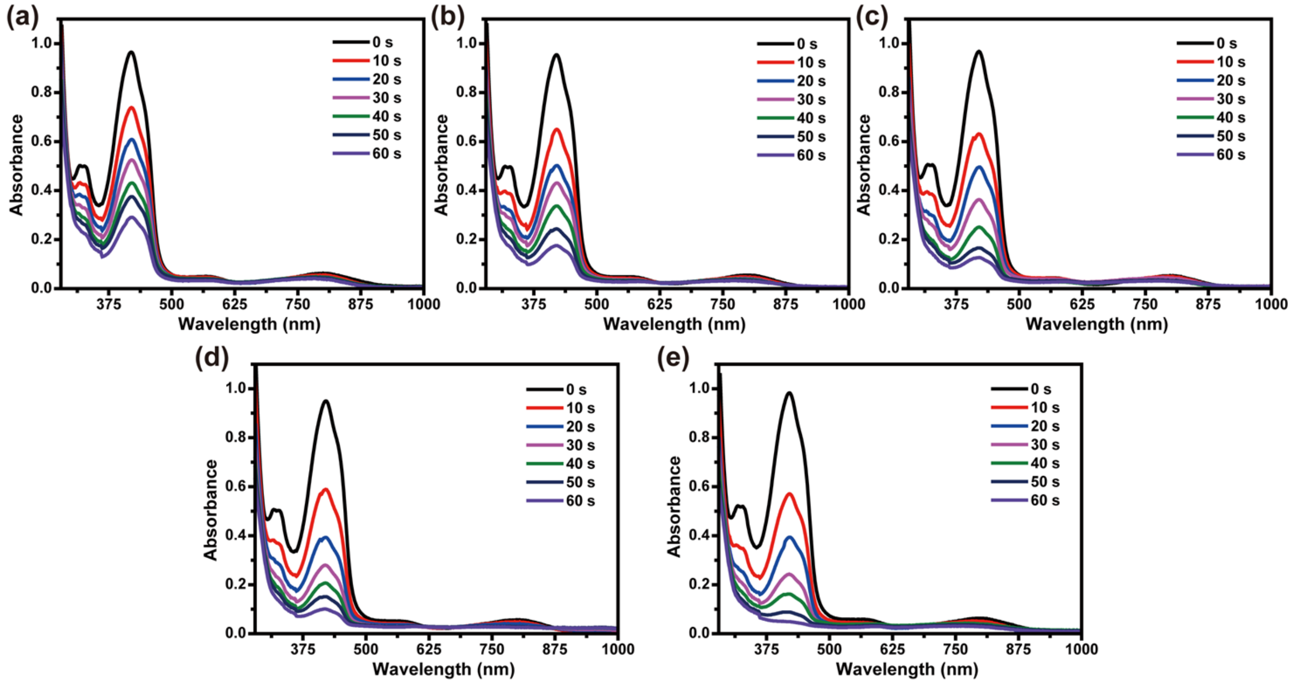

Fig. S24 UV-vis spectra of (a) 1 μM, (b) 2 μM, (c) 3 μM, (d) 4 μM and (e) 5 μM of BDPN NPs and DPBF in the presence of 808 nm laser irradiation (0.1 W cm^{-2}) at different times.

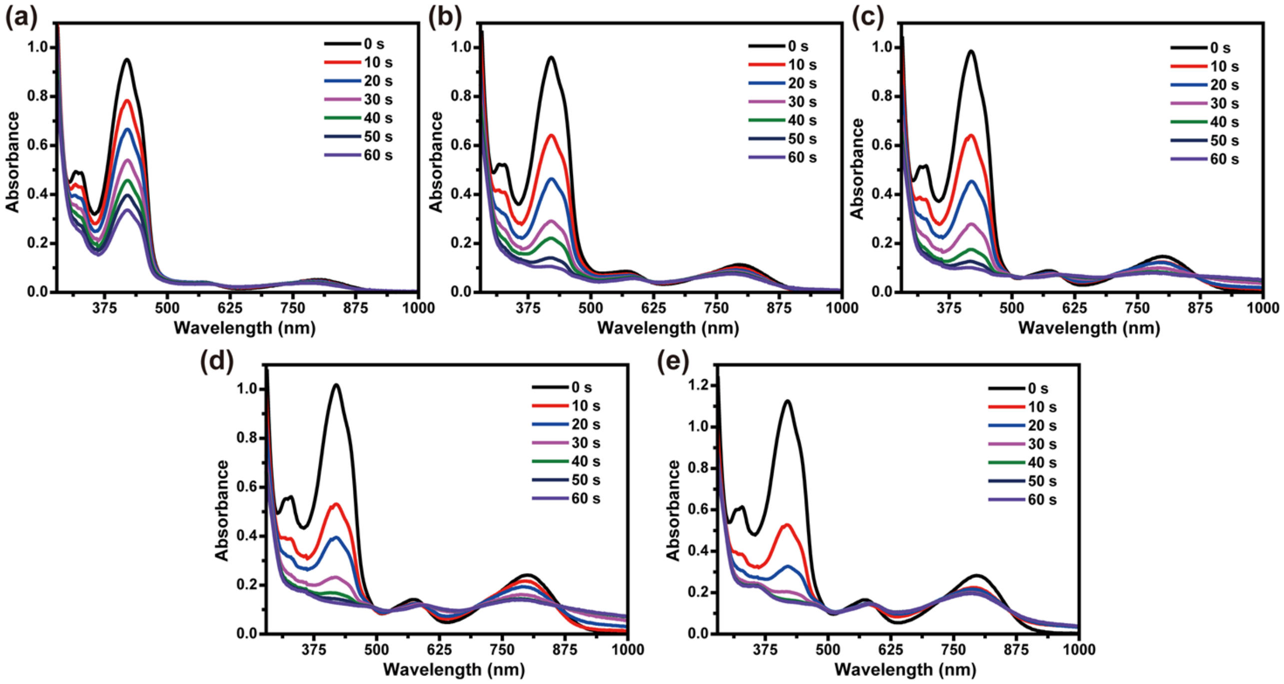

Fig. S25 UV-vis spectra of 5 μM of BDPN NPs and DPBF exposed to 808 nm laser with different powers ((a) 0.1 W cm^{-2}, (b) 0.2 W cm^{-2}, (c) 0.3 W cm^{-2}, (d) 0.4 W cm^{-2}, (e) 0.5 W cm^{-2}) for different times.

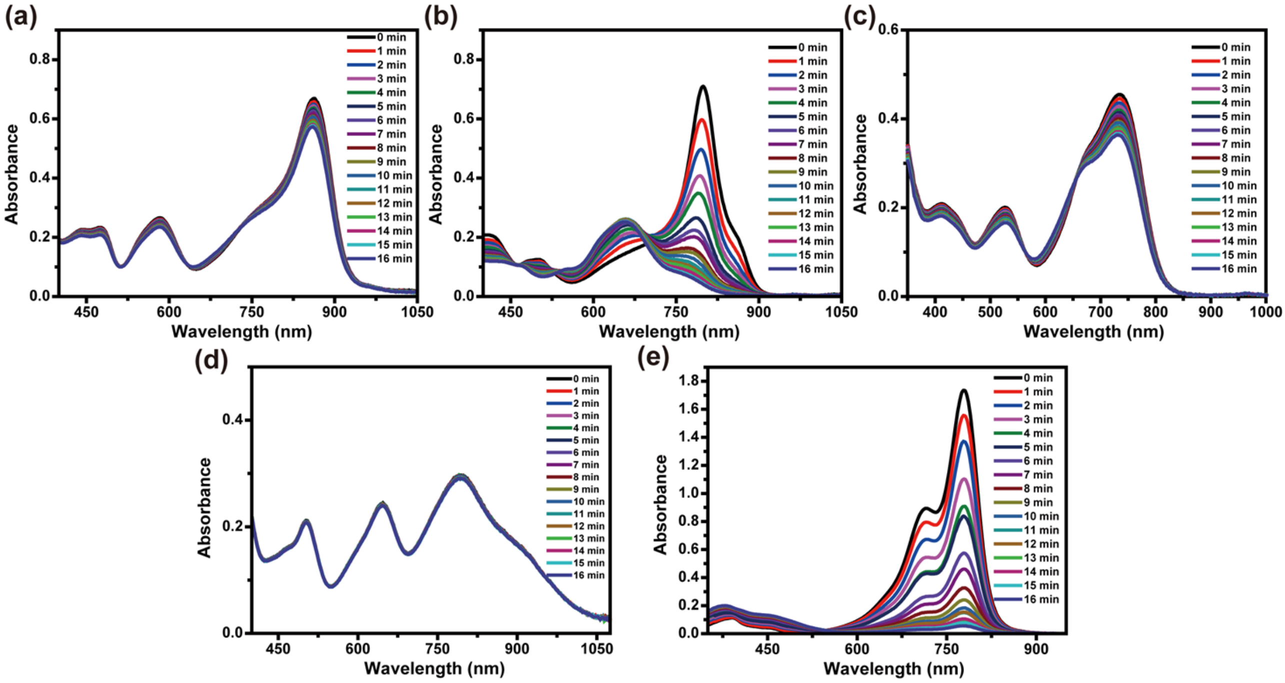

Fig. S26 UV-vis spectra of (a) BDPN NPs, (b) BDPI NPs, (c) BDPC NPs, (d) BDPJ NPs, (e) ICG, exposed to 808 nm laser (0.5 W cm^{-2}) for different times.

11. Singlet oxygen quantum yield

In order to quantitatively determine the ROS generation capacity of the four NPs, singlet oxygen quantum yield (Φ_Δ) was calculated using 1, 3-diphenylisobenzofuran (DPBF) as $^1O_2$ probe and indocyanine green (ICG) as reference (Φ_Δ = 0.14 in water)[S2]. The four NPs or ICG (50 μL, 20 μM) was dissolved in water (1880 μL), and then a solution of DBPF in THF (100 μL, 1 mM) was added. The mixture was exposed to 808 nm laser irradiation (0.1 W cm^{-2}). The absorbance of each mixed solution at 415 nm was recorded by UV-vis spectrophotometer in an interval of 10 s. Φ_Δ was calculated according the following equation:

$$\Phi_\Delta = \Phi_{\Delta \mathrm{ICG}} \times [k_{\mathbf{NPs}}/k_{\mathrm{ICG}}] \times [F_{\mathrm{NPs}}/F_{\mathrm{ICG}}]$$

Where $k_{\mathbf{NPs}}$ and k_{ICG} are the slopes of absorbance of DPBF (415 nm) under sample and ICG treatment as a function of irradiation time, respectively. F stands for the absorption correction factor, which is given by F = 1 – $10^{-\mathrm{OD}}$ (OD represents the optical density of NPs and ICG at 808 nm).

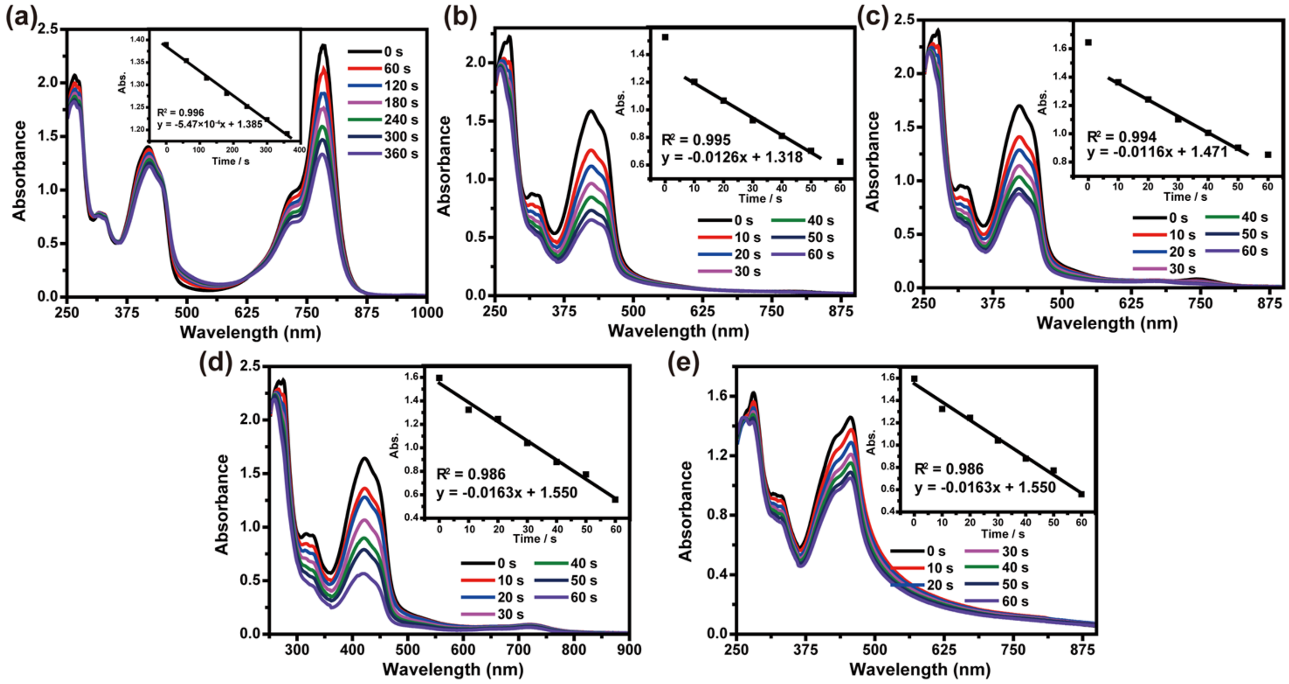

Fig. S27 UV-vis absorption changes of (a) ICG, (b) BDPN NPs (c) BDPI NPs, (d) BDPC NPs, (e) BDPJ NPs using DBPF as a probe upon irradiation (808 nm, 0.1 W cm^{-2}) (Inset: Linear fitting of absorption changes of DPBF at 415nm).

12. Photothermal effect and photothermal conversion efficiency

The temperature changes of four NPs (30 μM) were recorded by a thermal imager under 808 nm laser irradiation (0.5 W cm^{-2}) at one minute intervals. The solutions of BDPN NPs at the concentrations of 0, 10, 20, 30, 40 and 50 μM were irradiated for 10 min by 808 nm laser (0.5 W cm^{-2}). The solutions of BDPN NPs (20 μM) were irradiated for 10 min by 808 nm laser at different power levels of 300, 500, 700 and 900 mW cm^{-2} for 10 min. The temperature of each solution was recorded every 1 minutes using a thermal imager.

The temperature rise and natural cooling of NPs irradiated by 808 nm laser (0.5 W cm^{-2}) for 5/10 min were recorded by a thermal imager. The photothermal conversion efficiency was calculated according to Equation (1), and other parameters in Equation (1) can be calculated from Equations (2), (3) and (4).

$$\eta = \frac{\mathrm{hs}(T_{\max} - T_{sur}) - Q_{Dis}}{\mathrm{I}(1\text{-}10^{-\mathrm{A}_{808}})} \quad (1)$$

$$\theta = \frac{T - T_{\mathrm{sur}}}{T_{\max} - T_{sur}} \quad (2)$$

$$\mathrm{t} = -\tau_s \ln(\theta) \quad (3)$$

$$\mathrm{hs} = \frac{m_D C_D}{\tau_s} \quad (4)$$

Where η is the photothermal conversion efficiency, h is the heat transfer coefficient, s is the surface area of the container. $T_{\max}$ and T_{sur} are the highest temperature of four NPs at the highest steady-state temperature in water and the environmental temperature, respectively. I is the laser power density (0.5 W cm^{-2}) and A_{808} is the absorbance of four NPs at 808 nm. Q_{Dis} is the heat dissipated by the light absorbed by the solvent and the container. τ_{s} is the time constant. m_{D} is the mass of the solution containing the sample and C_{D} is the specific heat capacity of the solution (C_{water} = 4.2 J/g·°C)$^{\mathrm{S3}}$.

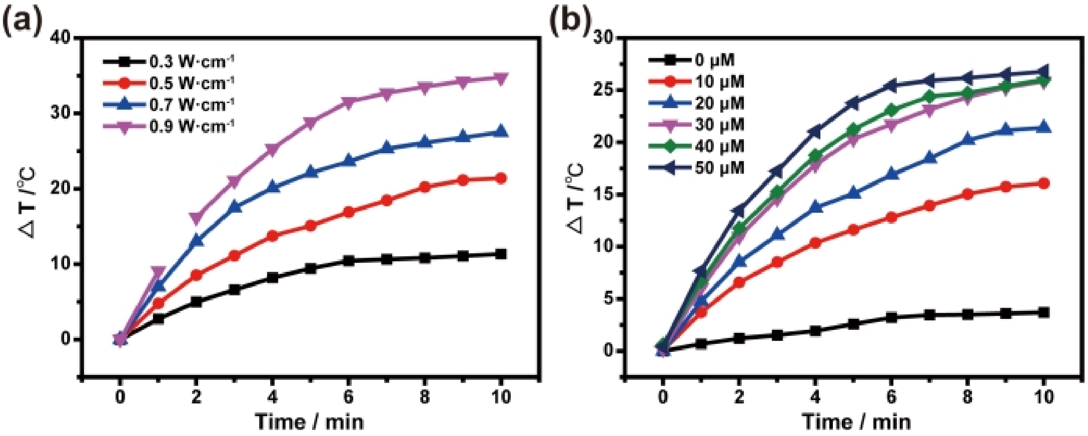

Fig. S28 (a) Photothermal property of BDPN NPs (20 μM) by 808 nm laser irradiation at different power densities (0.3-0.9 W cm^{-2}). (b) Photothermal property of different concentrations of BDPN NPs irradiated by 808 nm laser (0.5 W cm^{-2}).

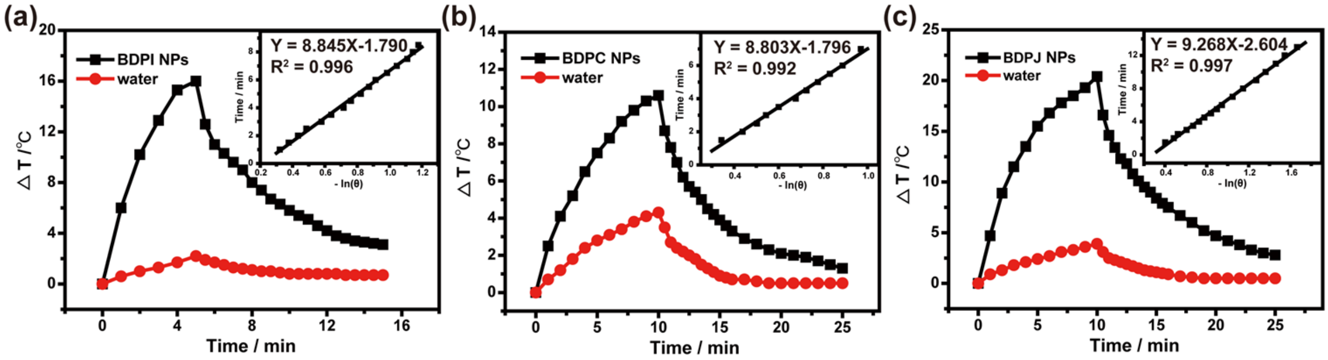

Fig. S29 Temperature curves of (a) BDPI NPs (b) BDPC NPs (c) BDPJ NPs (30 μM) exposed to 808nm laser for 5 or 10 min and subsequently without laser irradiation (Inset: Linear fitting of $-\ln\theta$ and time of NPs).

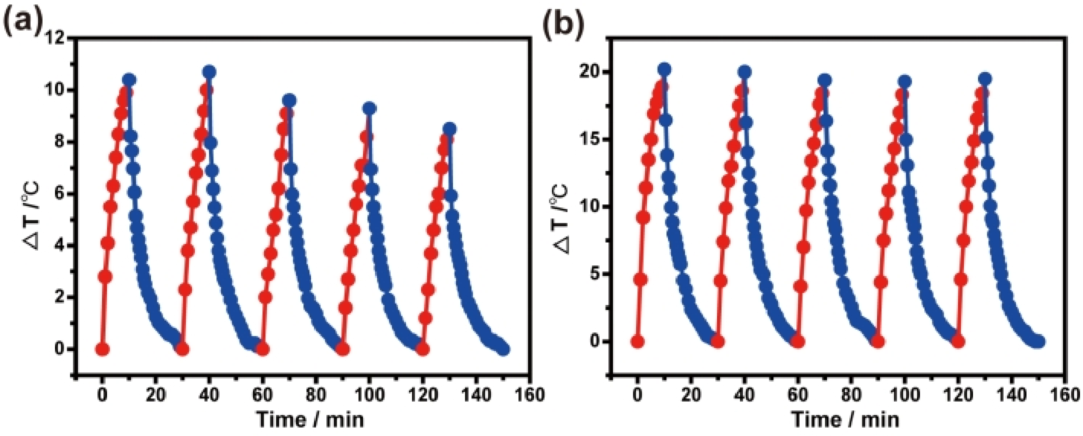

Fig. S30 Photothermal stability study of (a) BDPC NPs and (b) BDPJ NPs (30 μM) during five heat-cooling circles.

Table S2 Photophysical and photosensitizing properties of BDP dyes.

	λ_{abs} / nm (CH_2Cl_2)	λ_{em} / nm (CH_2Cl_2)	$\varepsilon\times10^4$ / M^{-1} cm^{-1} (CH_2Cl_2)	λ_{abs} / nm (NPs)	λ_{em} / nm (NPs)	$\varepsilon\times10^4$ / M^{-1} cm^{-1} (NPs)	FLQY (CH_2Cl_2)	FLQY (NPs)	ROS yield	PCE
BDPN	755	853	9.64	860	910	8.36	12.75%	3.0%	40.76%	54.9%
BDPI	724	773	4.17	798	877	4.96	24.34%	2.0%	46.88%	23.36%
BDPC	698	739	8.31	737	804	4.93	25.32%	1.52%	88.23%	21.45%
BDPJ	791	924	3.42	800	1043	2.08	5.95%	1.26%	9.33%	30.07%

13. Cell culture, Cellular uptake and flow cytometry

The mouse breast cancer cells (4T1 cells) were cultured in Dulbecco's modified Eagle medium (DMEM) containing 10% fetal bovine serum (FBS), 1% penicillin and streptomycin under a humidified atmosphere with at 37 °C in a humidified incubator with 5% CO_2.

Cellular uptake of NPs was examined by confocal laser scanning microscopy (CLSM). 4T1 cells were seeded onto 24-well plates (4×10^4 cells/well). After 18 h of culture, each well was treated with BDPN NPs (1.0 μg mL^{-1}), BDPC NPs (1.0 μg mL^{-1}) and BDPJ NPs (1.0 μg mL^{-1}), respectively. The culture medium was removed after 4 h incubation, then the cells were washed twice with PBS, and fixed with 4% formaldehyde for 10 min. Subsequently, formaldehyde was removed, and then the cells were washed 2~3 times with PBS, and the cell nucleus were stained with 4', 6-diamidino-2-phenylindole (DAPI, 500 μL/well) for 8 min to assist development. The confocal images were acquired on a CLSM (Radiance 2100, Bio-Rad).

Flow cytometry was used to investigate the uptake of NPs over time. 4T1 cells were seeded onto 12-well plates (8×10^4 cells/well). After 18 h of culture, each well was treated with only culture medium, BDPN NPs, BDPC NPs and BDPJ NPs (1.0 μg mL^{-1}) for 1 h, 2 h, 4 h and 8 h, respectively. Then, the culture medium was removed, and the cells were washed twice with PBS. Finally, the cells were harvested and analyzed by flow cytometer (CytoFLEX S, Beckman Coulter).

14. MTT assay

The cytotoxicity of BDPN NPs, BDPC NPs and BDPJ NPs was evaluated by 3-(4,5-dimethythiazol-2-yl)-2,5-diphenyltetrazolium bromide (MTT) assay. 4T1 cells were seeded in four 96-well plates at a density of 1×10^4 cells/well. After 18 h of culture, the medium was removed and the DMEM with different concentrations of BDPN NPs, BDPC NPs and BDPJ NPs was added to the well. After 4 h, one plate was irradiated with 808 nm laser irradiation (1.0 W cm^{-2}) for 3 min, and the other plate was placed in the dark for the same time as control. After 24 h of incubation, MTT solution (500 μg mL^{-1}) was used to replace the medium again, incubated for 4 h, and then replaced with 100 μL of DMSO per well. Subsequently, the absorbance at 570 nm was monitored by the enzyme-labeled instrument (DNM-9602). Relative cell viability was calculated according to the following formula:

$$\text{Cell viability (\%)} = A_{\text{experimental}}/A_{\text{control}} \times 100\%$$

To evaluate its photodynamic and photothermal effects at the cellular level, one plate of 4T1 cells was incubated with VC (1 mM) and different concentrations of NPs, followed by laser irradiation, and the other plate was incubated with different concentrations of NPs only and subjected to laser irradiation at -4 °C. Finally, the survival rates of the two plates were monitored by MTT assay.

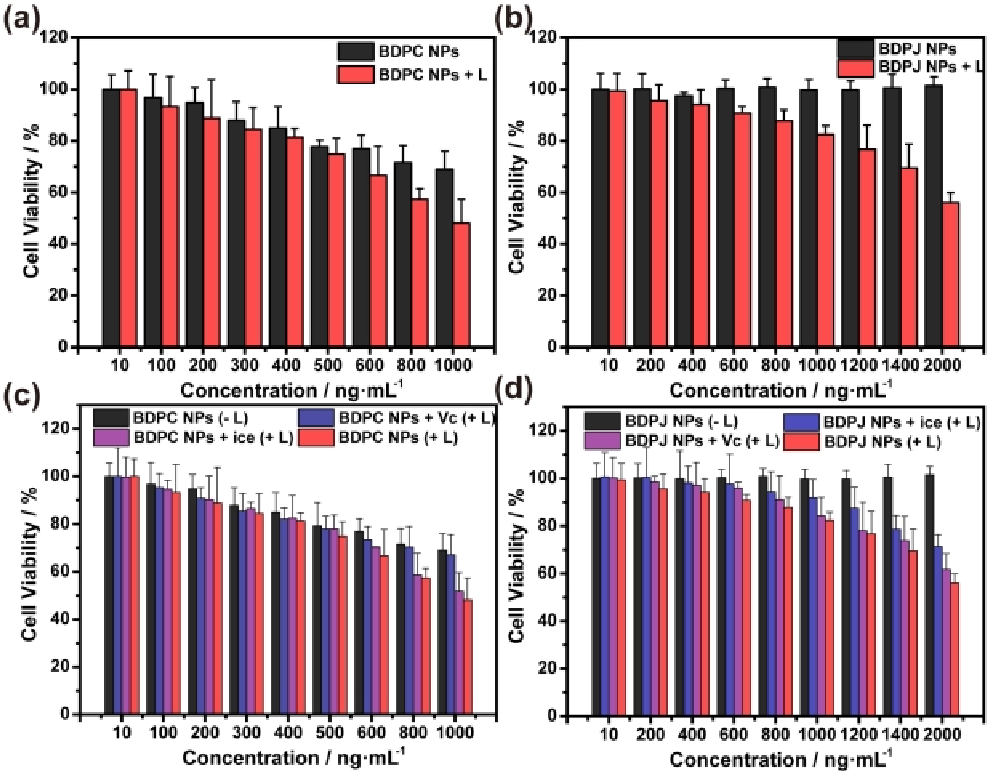

Fig. S31 Cell viability of 4T1 cells treated with (a) BDPC NPs and (b) BDPJ NPs under laser irradiation or darkness. Cell viability of 4T1 cells treated with (c) BDPC NPs and (d) BDPJ NPs with laser irradiation or darkness, or NPs with light irradiation together with VC (1 mM) or ice bath.

15. Intracellular ROS detection

2', 7'-Dichlorodihydrofluorescein diacetate (DCFH-DA) was used as an index to detect intracellular ROS generation. 4T1 cells were seeded in 24-well plate at a density of 4×10^4 cells/well. After 18 h of culture, each well was treated with only culture medium, BDPN NPs (0.4 μg mL^{-1}), BDPC NPs (0.4 μg mL^{-1}) and BDPJ NPs (0.4 μg mL^{-1}). Then, the medium was removed and DCFH-DA (10 μM) was added and incubated for 30 min. Two more washes were performed with PBS. Its fluorescence imaging was observed under dark or 808 nm laser irradiation (1.0 W cm^{-2}) for 3 min, and recorded with the inverted fluorescence microscope (Nexcope NIB610-FL).

16. Live/dead cell staining assay

Live/dead cell staining assay was performed with calcein acetoxymethyl ester (calcein AM) and propidium iodide (PI). 4T1 cells were seeded in 24-well plate at a density of 4×10^4 cells/well. After 18 h of culture, each well was treated with only culture medium, BDPN NPs (0.6 μg mL^{-1}), BDPC NPs (0.6 μg mL^{-1}) and BDPJ NPs (0.6 μg mL^{-1}). After 4 h, the wells irradiated with 808 nm (1.0 W cm^{-2}) laser light were used as the light group, and the remaining wells were placed in the dark as the control group. After 24 h of incubation, the cells were washed twice with PBS, stained with calcein AM and PI, and then washed with PBS twice to remove residual dye. The green fluorescence of Calcein AM representing live cells and the red fluorescence of PI representing dead cells were observed with the inverted fluorescence microscope (Nexcope NIB610-FL).

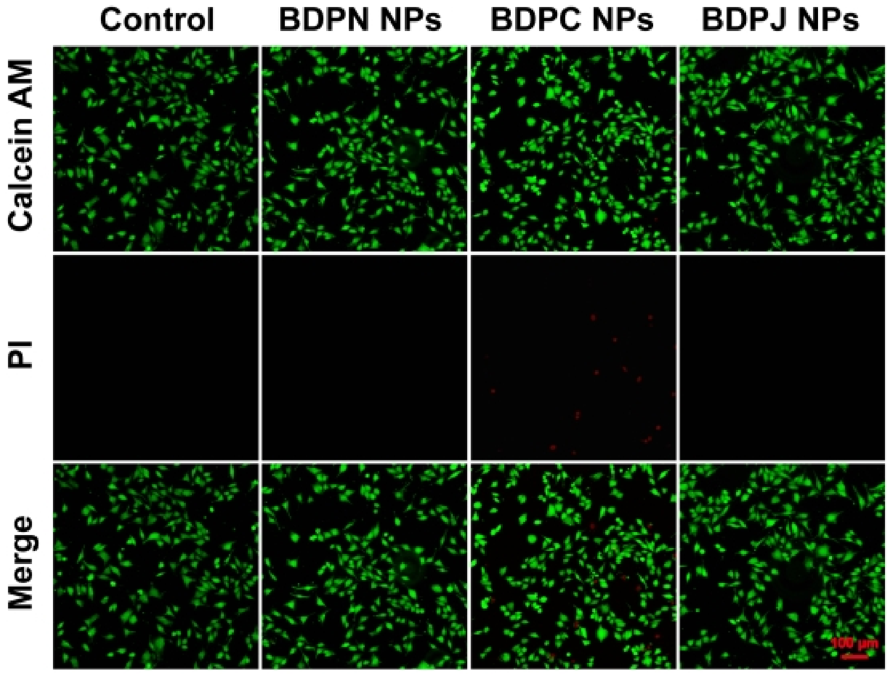

Fig. S32 Live/dead costaining images of 4T1 cells treated with three NPs (0.6 μg mL^{-1}) without laser irradiation. All the scale bars are 100 μm.

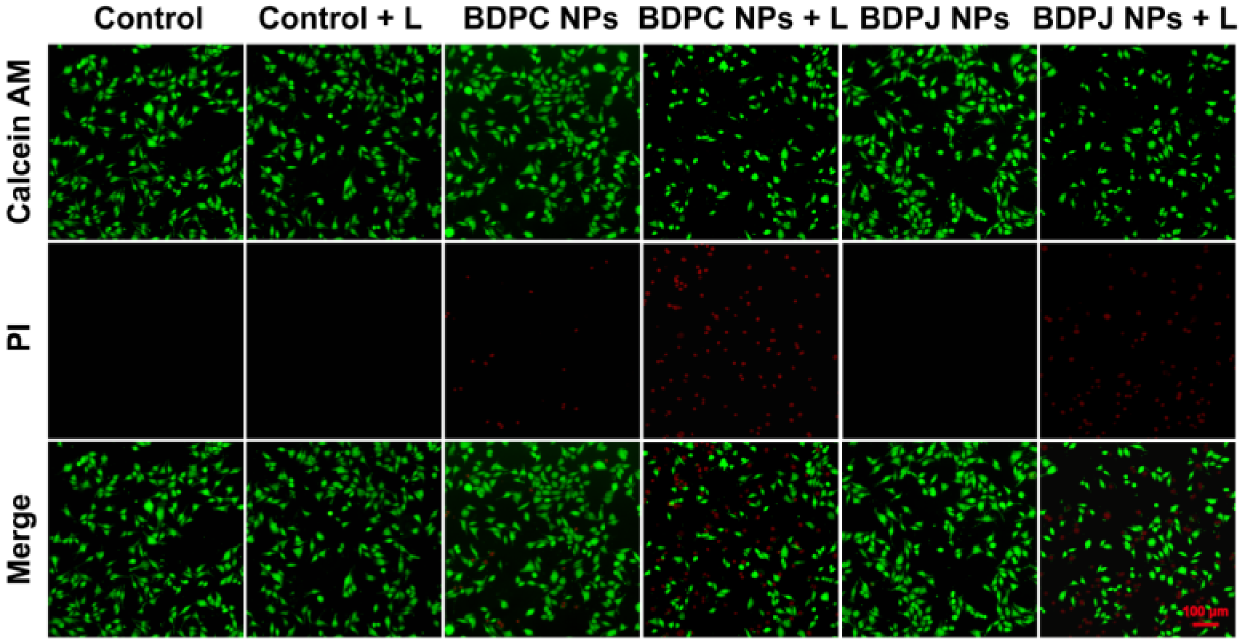

Fig. S33 Live/dead costaining images of 4T1 cells treated with BDPC NPs (1 μg mL^{-1}) and BDPJ NPs (2 μg mL^{-1}) with and without laser irradiation (808 nm, 1.0 W cm^{-2}). All the scale bars are 100 μm.

17. Mitochondria damage assay

JC-1 is used as a probe to detect changes in mitochondrial membrane potential for early apoptosis detection. 4T1 cells were seeded in 24-well plate at a density of 4×10^4 cells/well. After 18 h of culture, each well was treated with only culture medium, BDPN NPs (0.6 μg mL^{-1}), BDPC NPs (1.0 μg mL^{-1}) and BDPJ NPs (2.0 μg mL^{-1}). After 4 h, the wells irradiated with 808 nm (1.0 W cm^{-2}) laser light were used as the light group. After 24 h of incubation, the cells were washed twice with PBS, stained with JC-1 for 20 min. The confocal images were acquired on a CLSM (Radiance 2100, Bio-Rad).

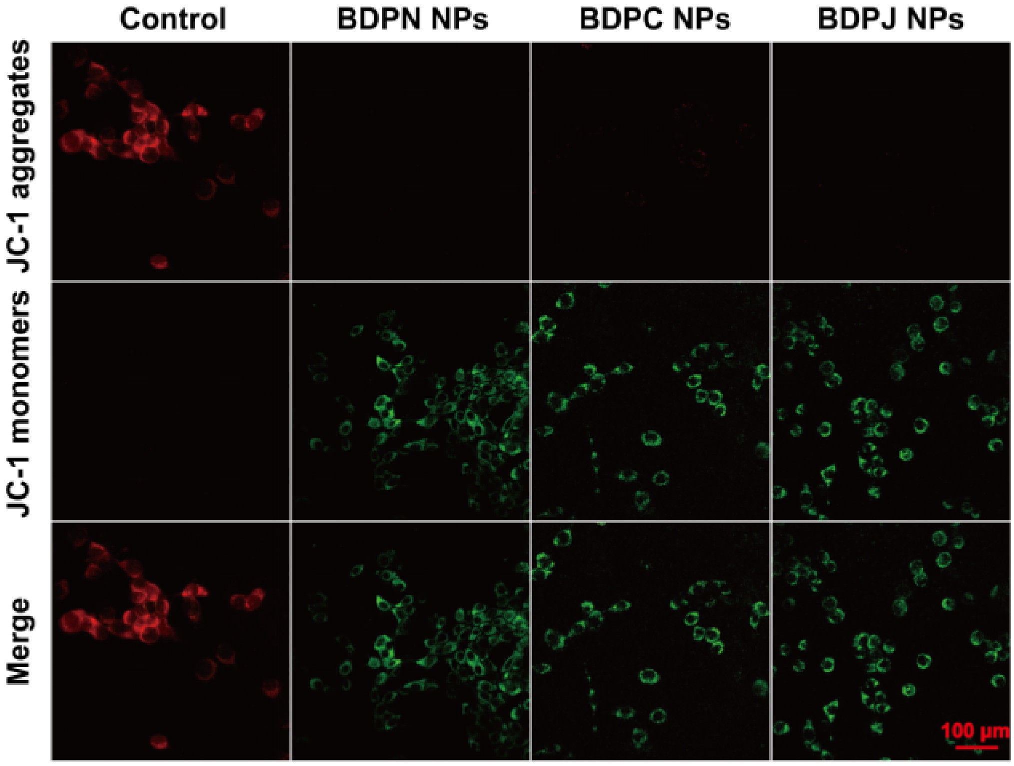

Fig. S34 JC-1 costaining images of 4T1 cells treated with BDPN NPs (0.6 μg mL^{-1}), BDPC NPs (1 μg mL^{-1}) and BDPJ NPs (2 μg mL^{-1}) with 808 nm laser irradiation (1.0 W cm^{-2}, 3 min). All the scale bars are 100 μm.

18. Tumor mouse model

BALB/c mice (6 weeks old, weighting about 20 g) were purchased from Laboratory Animal Center of Hangzhou Normal University. They were cultured in a pathogen-free environment with appropriate humidity and temperature. All animal manipulations were performed in accordance with Chinese Animal Protection Network (CAPN). The tumor-bearing mice were prepared by subcutaneously injecting 100 μL of PBS containing 10^6 4T1 single cell suspension into the back of nude mice bearing tumor. After 6 days, the mice bearing 4T1 tumors (average volume about 100 mm^3) were treated by BDPN NPs, BDPC NPs or BDPJ NPs to observe the therapeutic effect.

19. In vivo fluorescence imaging, photoacoustic imaging and photothermal imaging

The tumor-bearing mice were injected with BDPN NPs, BDPC NPs and BDPJ NPs (30 μg mL^{-1}), respectively. Fluorescence imaging of BDPN NPs, BDPC NPs and BDPJ NPs using a 808 nm excitation filter and 900 nm emission filter were performed on a Monet IGS-1000 imaging system. Photoacoustic imaging of mouse tumor and imitation model were obtained. Photothermographic images of mouse tumor sites at different times were obtained by thermal imager.

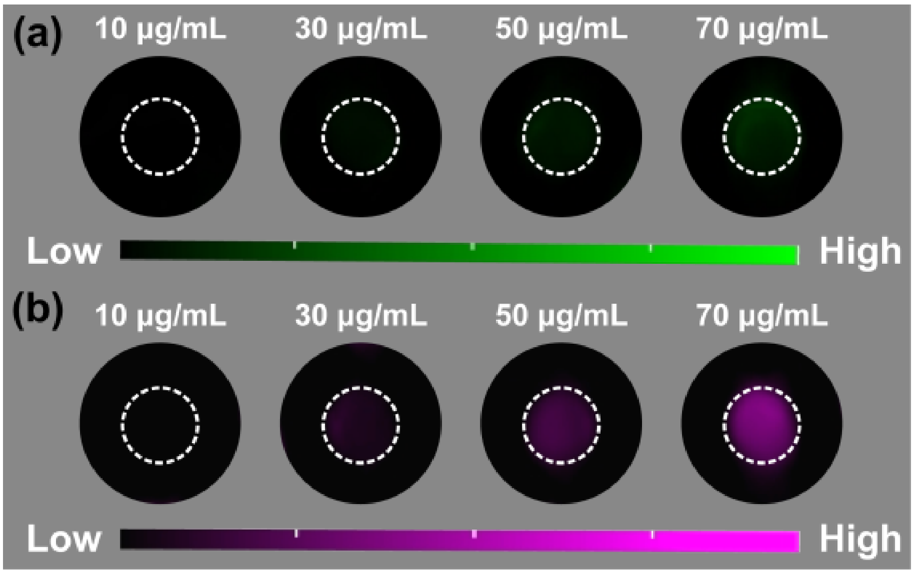

Fig. S35 Photoacoustic image of (a) BDPC NPs and (b) BDPJ NPs at different concentrations.

20. In vivo anticancer therapy

4T1 tumor-bearing mice were used for *in vivo* anticancer therapy. The mice were randomly divided into 8 groups with 6 mice in each group: Group 1: injected with 100 μL PBS only; Group 2: injected with 100 μL PBS + laser; Group 3: injected with 100 μL BDPN NPs (0.15 mg kg^{-1}); Group 4: injected with 100 μL BDPN NPs (0.15 mg kg^{-1}) + laser; Group 5: injected with 100 μL BDPC NPs (0.15 mg kg^{-1}); Group 6: injected with 100 μL BDPC NPs (0.15 mg kg^{-1}) + laser; Group 7: injected with 100 μL BDPJ NPs (0.15 mg kg^{-1}); Group 8: injected with 100 μL BDPJ NPs (0.15 mg kg^{-1}) + laser. The mice in the laser irradiation group were irradiated with 808 nm (1.0 W cm^{-2}) laser for 3 min, processed once every two days. The mice body weight and tumor volume were measured every two days until day 14.

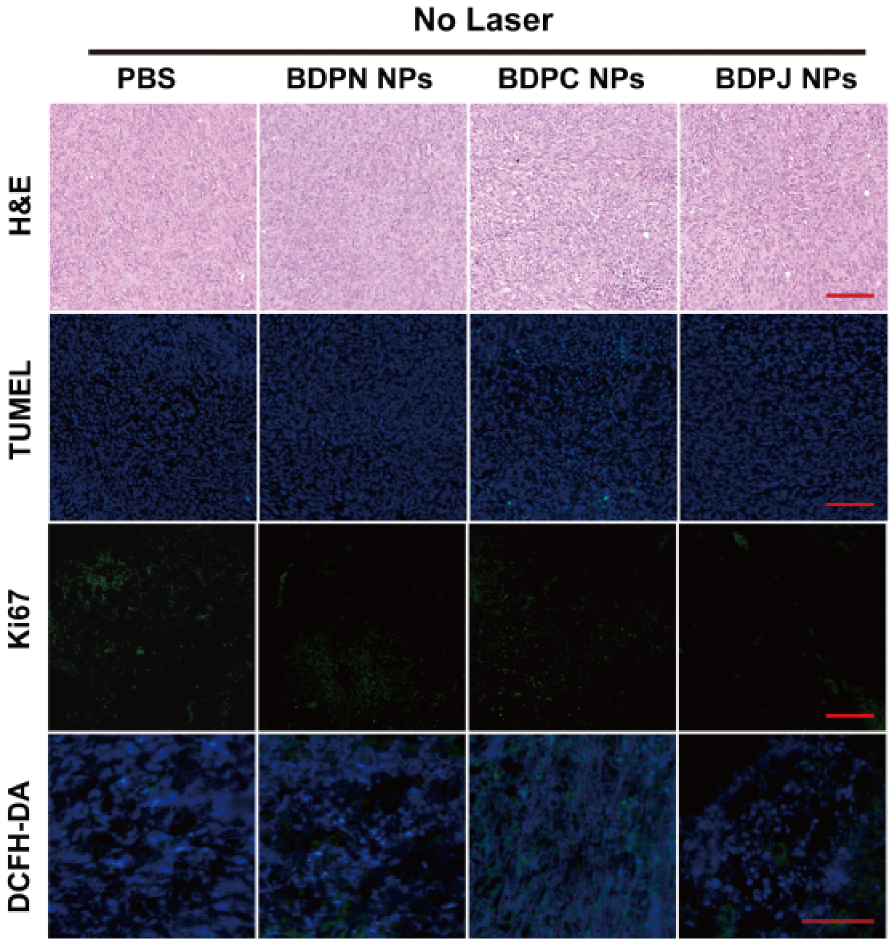

Fig. S36 H&E, TUNEL, Ki67 staining and DCFH-DA analysis of tumor sites from the 4T1 tumor-bearing mice treated with PBS, BDPN NPs, BDPC NPs and BDPJ NPs without laser irradiation, respectively. All the scale bars are 100 µm.

21. In vivo biological safe experiments

After the treatment, the tumor-bearing mice were sacrificed, the tumor and main organs (heart, live, spleen, lung, kidney) were dissected, and photos of the tumor were taken to visually observe the final treatment results. After the tissues were isolated and fixed with 4% paraformaldehyde, embedded in paraffin, and sliced with a thickness of 3 µm. Subsequently, they were stained with hematoxylin and eosin (H&E), Ki67 and TUNEL prior to histopathological analysis. At the moment, eyeball blood of mice was collected by enucleation of mouse eyes before sacrificed for further blood biochemistry and haematology analysis. The observed indexes were alkaline phosphatase (ALP), aspartate aminotransferase (AST), alanine aminotransferase (ALT) and urea nitrogen (BUN), red blood cells (RBC), white blood cells (WBC), haemoglobin (HGB), blood routine levers of haematocrit (HCT), mean corpuscular volume (MCV), blood platelet (PLT), mean corpuscular haemoglobin concentration (MCHC), mean corpuscular haemoglobin (MCH), mean platelet volume (MPV), red cell distribution width (RDW-CV), lymphocyte (LYMPH%), neutrophil (NEUT%).

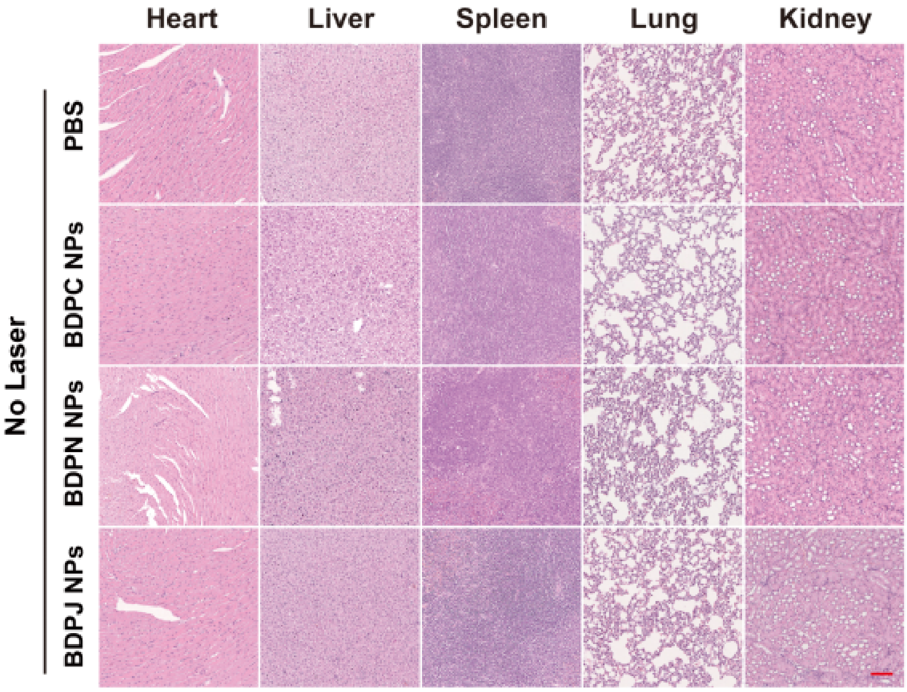

Fig. S37 H&E-stained tissue sections of major organs (including heart, liver, spleen, lung and kidney) from the mice in the no-laser irradiated experimental group. All the scale bars are 100 μm.

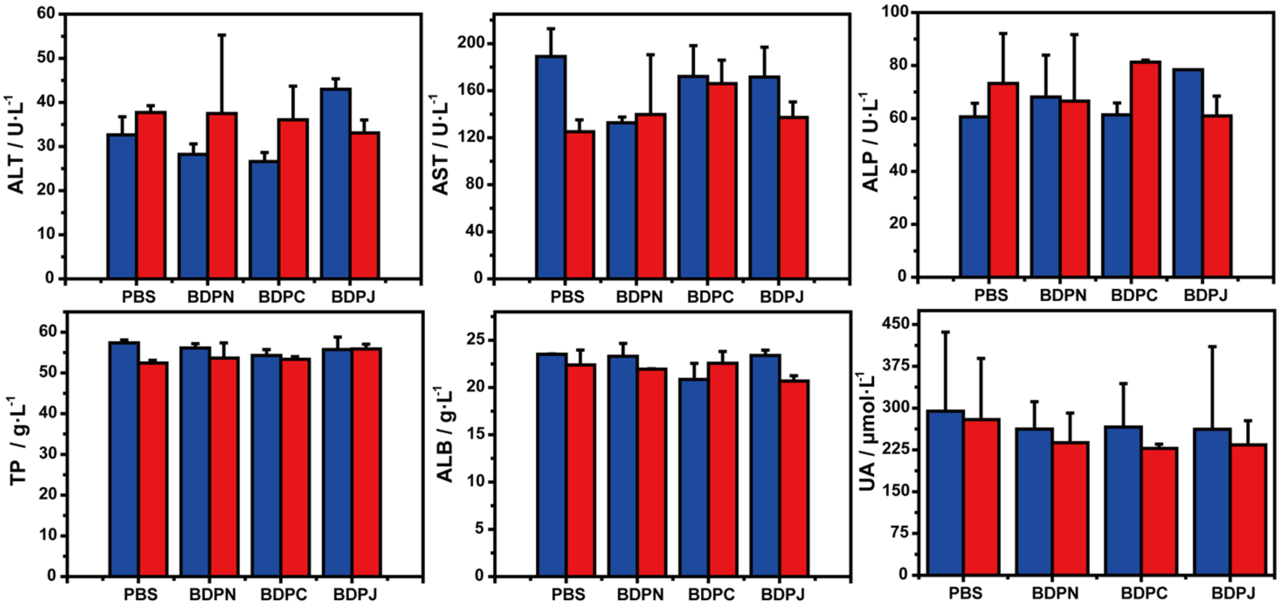

Fig. S38 The related indexes of blood biochemistry from the experimental mice after three NPs treatments. blue: drak, red: laser irradiation.

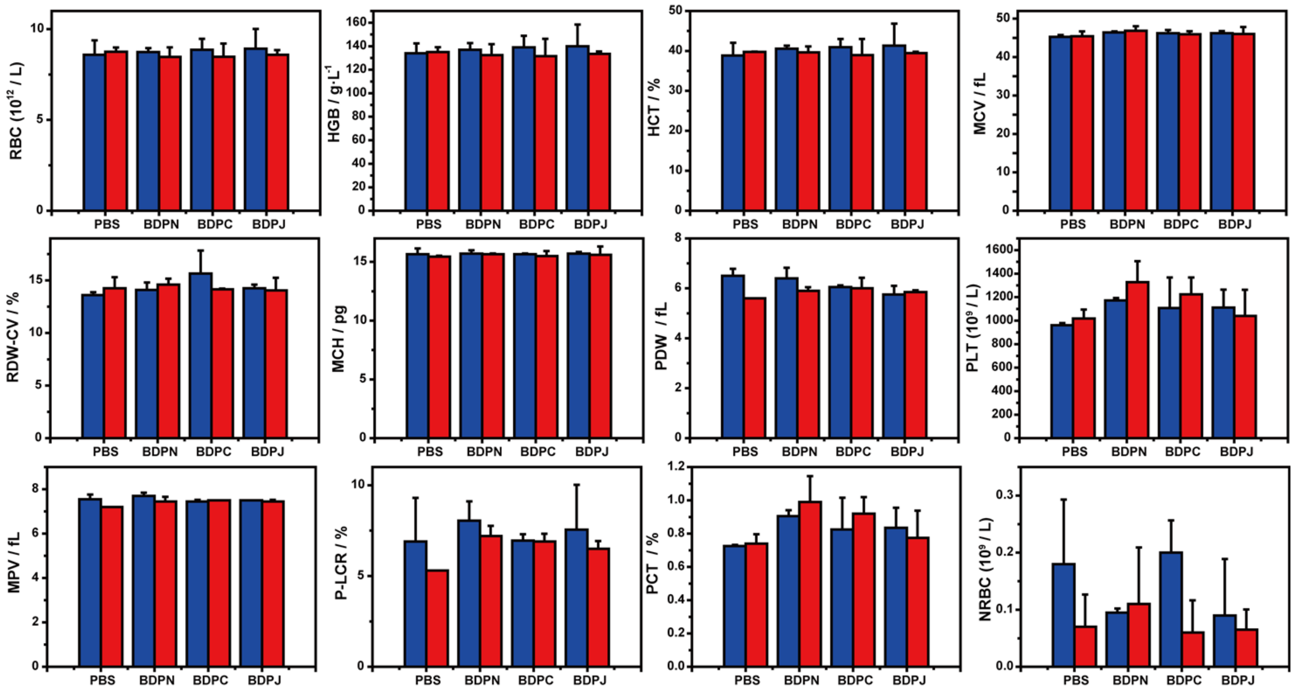

Fig. S39 The routine analysis of blood from the experimental mice after three NPs treatments. blue: drak, red: laser irradiation.

22. Reference

S1. J. Zhang, M. Jiang, Y. Li, J. Yu, H. Qiu, M. Gu, Y. Li and S. Yin, Self-assembled boron dipyrromethene-based nanocarriers with encapsulated doxorubicin for chemo-photodynamic therapy, *Dyes Pigm.* **2022**, *206*, 110679.

S2. T. Yang, L. Liu, Y. Deng, Z. Guo, G. Zhang, Z. Ge, H. Ke and H. Chen, Ultrastable near-infrared conjugated-polymer nanoparticles for dually photoactive tumor inhibition, *Adv. Mater.* **2017**, *29*, 1700487.

S3. X. Liu, B. Li, F. Fu, K. Xu, R. Zou, Q. Wang, B. Zhang, Z. Chen and J. Hu, Facile synthesis of biocompatible cysteine-coated CuS nanoparticles with high photothermal conversion efficiency for cancer therapy, *Dalton T.* **2014**, ***43***, 11709–11715.

---

[i] Neese, F. Software update: The ORCA program system—Version 5.0. WIREs Comput Mol Sci. 2022;e1606. https://doi.org/10.1002/wcms.1606

[ii] Rolfes, J. D.; Neese, F.; Pantazis, D. A. (2020) J. Comput. Chem., 41, 1842.